Nano-Structures & Nano-Objects 23 (2020) 100500

Contents lists available at ScienceDirect

Nano-Structures & Nano-Objects

journal homepage: www.elsevier.com/locate/nanoso

Self-healing polymers: Synthesis methods and applications

Kakarla Raghava Reddy [a,c,*], Abbas El-Zein [b], David W. Airey [b], Fernando Alonso-Marroquin [b], Peter Schubel [c], Allan Manalo [c]

[a] School of Chemical and Biomolecular Engineering, The University of Sydney, Sydney, NSW 2006, Australia
[b] School of Civil Engineering, The University of Sydney, Sydney, NSW 2006, Australia
[c] University of Southern Queensland, Centre for Future Materials (CFM), Toowoomba, QLD 4350, Australia

ARTICLE INFO

Article history:
Received 2 February 2020
Received in revised form 6 May 2020
Accepted 10 May 2020

Keywords:
Clays
Crack healing
Self-healing polymers
RAFT
ATRP
Click chemistry

ABSTRACT

Clays have numerous applications in a variety of applications including engineering, medical and civil areas. The wide applicability of clays is attributed to their useful physico-mechanical as well as biomedical applications, since they are readily available, nontoxic to human body and environment, low cost and having kneading, swelling, adsorption of properties for metal ions. Industrial sectors in different fields are greatly dependent on the usage of different clays, but the cracks or defects or damaged areas present in clays restrict their practical applications. In order to overcome these problems, various polymeric materials have been developed through different strategies to heal the cracks or repair the damaged areas of clays, and improve their properties and potential usage in various applications. This review will address several aspects such as preparation, structure–property relationships, properties of different types of clays and self-healing polymers, healing process of cracks in clays using polymers, crack healing mechanism, test methods of healing efficiency, properties (e.g. structure, hydraulic conductivity, swelling nature, mechanical and rheology) of clays before and after healing of cracks, and their applications.

Contents

1. Introduction 2
2. Classification and properties of clays 2
   2.1. Layered double hydroxides (LDHs) 2
   2.2. Montmorillonite (MMT) 2
   2.3. Sepiolite 3
   2.4. Brucite 3
   2.5. Zeolites 3
   2.6. Bentonite 3
   2.7. Preparation of clays 3
   2.8. Applications of clays 4
3. Chemistry of self-healing materials (design and synthesis methodologies) 5
   3.1. Intercalation strategies of polymers in the interlayer galleries of clays 5
   3.2. Self-healing strategies of polymers and its mechanism 5
      3.2.1. Photo-irradiation-assisted self-healing 6
      3.2.2. Microcapsule-based self-healing process 6
      3.2.3. Self-healing through reversible bond formation 6
      3.2.4. Controlled/living polymerization-driven self-healing 8
      3.2.5. Crack healing via molecular interdiffusion approach 11
      3.2.6. Layer-by-layer (LBL) assembly-assisted crack healing 11
      3.2.7. Polymer hydrogels for crack healing 11
      3.2.8. Recombination of chain ends-driven crack healing 13
      3.2.9. Nanostructured material-assisted self-healing 13

* Corresponding author at: School of Chemical and Biomolecular Engineering, The University of Sydney, Sydney, NSW 2006, Australia.
E-mail address: reddy.chem@gmail.com (K.R. Reddy).

https://doi.org/10.1016/j.nanoso.2020.100500

3.2.10. Mussel-inspired chemistry-assisted self-healing 13
3.2.11. Schiff base reactions based self-healing 14
4. Crack healing of clays and other inorganic solid materials using self-healing polymers 14
5. Assessment of healing efficiency of crack-healed system 16
6. Conclusions 16
Declaration of competing interest 16
Acknowledgment 16
References 16

1. Introduction

Clays are widely used inorganic materials owing to their low cost, nontoxicity, ready availability in nature, good thermal and environmental stability, hardness, and excellent rheological properties. They have a wide range of potential applications in different research fields and industries such as medicine, cosmetics, steel making, ceramics, hydraulic engineering, infrastructural engineering, construction and building materials, surfacing roads, roofing, flooring, as single liners for canals or ponds, and adsorption and removal of heavy metal ions and hazardous compounds from contaminated water [1–4]. However, the presence of cracks in clays is a major issue that hinders their use for practical applications. Crack healing is important, because small cracks generate brittleness that causes deterioration in their properties [5–7]. Therefore, healing of cracks in damaged areas of clays has been an important topic of research in recent years.

Smart self-healing polymers have received much interest in recent years, owing to their ability to heal damaged material via scratching, or retaining their original physico-chemical and mechanical properties [8–10]. For developing well-defined organic polymers with self-healing properties, the polymers must have functionalities that can react with other groups. This necessitates the use of controlled polymerization reactions by combining suitable coupling reactions, such as embedding organic monomer molecules or catalysts or crosslinking agents such as organic monomers or catalysts or crosslinking agents into polymer matrix [11–15]. Among many self-healing methodologies, covalent bond formation is an effective approach for long-standing structural applications, because covalent linkages are quite strong between the healing agent and matrix, giving materials with remarkable strength. The healing of cracks, defects, or damages in clays by polymers is therefore important to improve the reliability and lifetime of clay minerals. To the best of our knowledge, there are no review reports focusing on the effects of cracks, as well as strategies used in healing/repairing cracks in clays.

This review addresses the fabrication methodologies and structural characteristics of different layered clay-based materials, and synthesis strategies of various self-healing polymers, their structure–property relationships. Self-healing process of cracks in different clays through self-healing polymers, crack-healing mechanisms, test methods of healing efficiency, properties (e.g., hydraulic conductivity, mechanical, and rheological) of crack-healed clays, and their advances in engineering areas are discussed.

2. Classification and properties of clays

Clay particles are inorganic species. Two types of clays as cationic clays, which are layers of aluminosilicates with negative charge, and anionic clays, which are hydroxide layers with positive charge. Based on the elemental composition, the primary component of clay is aluminum silicate, and the secondary components are apatite, zircon, granite, and others. Some of the primary groups of clay minerals are: (i) kaolinite (hydrated Al silicate), (ii) haloizit (hydrated Al silicate), (iii) Na-montmorillonite (hydrated silicates of mixed Al, Mg, and Na), (iv) illite (hydrated silicates of mixed Al, Fe, Mg, and Na), and several other types of pristine clays within these groups [16,17].

Clays play a vital role in industrial sectors due to their unique physical, mechanical, and rheological properties. The transport characteristics within clays could be improved by delamination, which provides channels within the matrix and this occurs by pillaring mediators (silicate, alumina), smaller particles (montmorillonite (MMT)) to obtain nanoporous structured clays, or by the insertion of organic molecules (polymers or surfactants).

2.1. Layered double hydroxides (LDHs)

Layered double hydroxides (LDHs), also known as anionic clay minerals or layered hydroxyl salts, are biocompatible. Hydrotalcite (Mg–Al–CO_3) is a mineral of this family with a similar isomorphic structure. Because hydrotalcite consists of hydroxycarbonate of magnesium and aluminum, it can be easily crushed into a fine powder. Thin layer-like structure of this clay has the formula of $Mg_6Al_2(OH)_6CO_3H_2O$. Positive charges in hydrotalcite can be achieved by the replacement of Mg^{2+} ions by Al^{3+} ions.

LDHs are normally known as hydrotalcite-like material owing to the isomorphic substitution of Al^{3+} ions. LDHs are two-dimensional (2D) morphological structure-based clay minerals with ordered self-assembling layers that have a controllable volume of the interlayers and variable host/guest structures, which can be fabricated through a layer-by-layer (LBL) assembly process. LDHs have a similar structure to brucite, consisting of layers with positive charge and charge-neutralizing anions, and solvent molecules inside the interlayer galleries. The general divalent cations (M^{2+}) of LDHs are Mg^{2+}, Zn^{2+}, Co^{2+}, Ca^{2+}, Cd^{2+}, Cu^{2+}, and Ni^{2+}, whereas trivalent cations (M^{3+}) cations are Al^{3+}, Cr^{3+}, and Fe^{3+}. Low-dimensional structured nanosheets of LDHs are formed by placing of metal cations in the centers of edge-sharing octahedra, where each metallic cation consists of six hydroxyl ions at the corners [18].

The unique and fascinating characteristics of LDHs such as the well-ordered structures, molecular self-aggregation inside the interlayer galleries, high thermal stability, ability to intercalate different types of species (e.g., inorganic, organic, and biomolecules), and simple LBL fabrication process render them highly attractive for potential applications in optics, separation technology, nanomaterial engineering, medicine, and catalysis. In particular, biocompatible characteristics of LDHs allow the clay to monitor, identify, and treat many diseases in a modestly invasive mode.

2.2. Montmorillonite (MMT)

MMT belongs to the smectite clay group, has tremendous intercalation properties, robust adsorption, and elevated affinity to organic molecules and heavy metals owing to its intrinsic inorganic 2D layered nanostructure, as shown in Fig. 1 [19]. With a strong pre-concentration ability, high cation exchange capability, and a peculiar layered structure, MMT has attracted much attention. MMT has some unique characteristics such as low price, good stability to chemicals, strong absorption, good

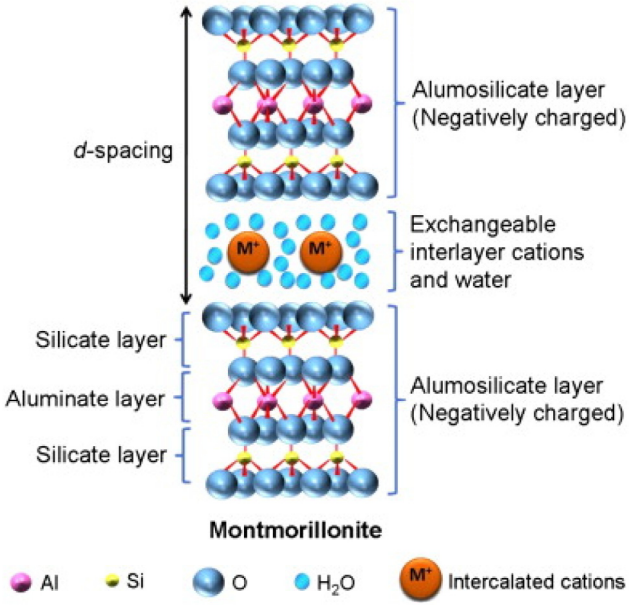

Fig. 1. Layered structure of Na-MMT. *Source:* Reprinted with permission from Ref. [19].

electron transport properties, and controllable structural properties. A subgroup of MMT is bentonite clay, which has applications in electrochemical sensors for the detection of organic molecules, cations, and adsorbents [20].

2.3. Sepiolite

Sepiolite clay ($Si_{12}O_{30}Mg_8(OH,F)_4(H_2O)_4.8H_2O$) is a fibrous clay and used as filler to strengthen the polymer mass. They do not have ability to mix, but provide interesting features such as high surface area and microporosity. Its morphological structure consists of octahedral magnesium oxide planes sandwiched between 3D nanosheets of tetrahedral silicates. The anionic and cationic charges on the surface and between the inner layers provide excellent absorption properties for heavy metal ions and polar organic materials. The presence of hydroxyl groups (Si–OH) at the exterior surface permits for easy functioning by the controlled modification via chemical reactions, e.g., by the attachment of nanoparticles or with binding agents [21].

2.4. Brucite

Brucite is a layer-like structured magnesium hydroxide [$Mg(OH)_6$)], in which divalent M^{2+}ions are octahedrally bounded by the hydroxide ions. These octahedral units share their edges and generate infinite layers in which hydroxyl (OH) form chemical bonds to the nanolayers. These OH anions are well-ordered in a highly packed 2D structured planes. The octahedral holes of hydroxyl planes are conquered by magnesium ions, resulting in a neutral layer. The elemental composition can change structure of brucite clay through the isomorphic replacement of divalent cations (M^{2+}) with trivalent cations (M^{3+}) [22].

2.5. Zeolites

Zeolites are crystalline microporous aluminosilicates, characterized by normalized spatial arrangement of tetrahedral TO_4 (T = Al, Si), leading to an improved structural arrangement consisting of homogeneous cavities, cages, or 3D networks (usually in the range of 4–15 Å), with maximum and minimum diameters that can easily distinguish molecules with dimensional variation < 1 Å. The replacement of Si^{IV} by Al^{III} in the network makes the whole moiety negatively charged in order to maintain electrical neutrality. The Si/Al ratio in the zeolite frame is related to its ion-exchange capacity and hence, these exhibit ion-exchanging ability and selectivity that make them special materials for electrochemical modifications [23].

2.6. Bentonite

Bentonite is a clay mineral that is a phyllosilicate with tetrahedral–octahedral–tetrahedral molecular structure (T–O–T morphology), as shown in Fig. 2 [24], whose the mineral composition is primarily dominated by negatively surface charged Na-MMT (smectite group). The common color of bentonites is pale-green, but they do occur with other colors (e.g., yellow, brown, red, etc.), based on the types of cations present. Bentonites have potential applications in the geo-environmental field to separate pollutants, owing to their low permeable properties (permeate with water) [25], which is dependent on low hydraulic conductivity (κ) of Na-MMT, as it is primary mineral component of bentonite clay [26]. It can be used alone or as a modified-natural soil. geosynthetic clay liners (GCLs, $\kappa = 10^{-11}$ m/s) consist of thin layers of bentonite clay sandwiched between two geo-textiles or strongly connected to a geo-membrane, and are utilized as hydraulic and gas barriers in landfills, contaminated mining waste, and other contaminated sites. GCLs containing bentonite clays have limited thickness, low price, low permeation, very low hydraulic conductivity to distilled water, high swelling nature, capacity of exchangeable cations, ability to withstand different environments, and excellent self-healing characteristics that are adversely affected by the desiccation and cracking in the bentonite [27–29].

Pure bentonite is unstable to chemicals and reactive in aqueous environments. Thus, high-performance engineered hydraulic barriers (low hydraulic conductivity) used in landfills require frequent inspection of its hydraulic activity, which has hydraulic conductivity parameter. An efficient hydraulic barrier with low values of κ avoids the penetration of water via this hydraulic barrier. Various parameters such as the mineral composition present in bentonite clay, cation locations in the clay, exposure to chemicals, pore fluid, and leakage water containing soluble minerals affect the characteristics [e.g., hardness, density, surface properties (surface area), wetting nature, swellability, thixotropy, cation exchange capacity, cohesiveness, sealing, binding with inorganic and organic compounds, etc.] of bentonite. Several types of bentonite are available based on the elemental composition, such as K, Na, Ca, and Al, and the most common types for industrial applications are Na- and Ca-based bentonites. The properties of some of the clays are given in Table 1.

2.7. Preparation of clays

Clay minerals (LDHs, MMTs, etc.) are prepared using various strategies such as chemical co-precipitation, ion exchange, reconstruction, and sol–gel processes. Among them, the chemical co-precipitation technique is most frequently used for one-step large-scale direct synthesis of clays (e.g., LDHs) with a wide range of divalent and trivalent cations and various anions (e.g., CO_3^-, NO_3^-, and Br^-), and different types of organic dyes and polymers have been intercalated. In this method, both the divalent and trivalent cations along with most of the anions to be intercalated are reacted in an aqueous system, followed by slowly increasing the pH value of the mixed solution through the addition of

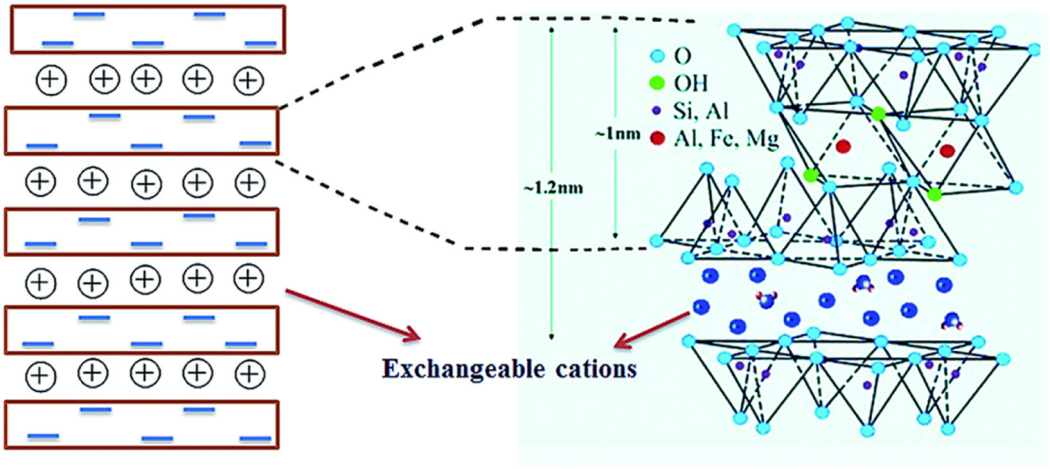

Fig. 2. Structure of bentonite clay.
Source: Reprinted with permission from Ref. [24].

Table 1
Physico-chemical characteristics of various clay minerals.

Property	Halloysites	Diatom materials	Platy clays	Zeolites	Other type clay minerals	Reference
Chemical composition	Mixture of Al and Si elements	Mainly SiO_2, < 10% of Al_2O_3 and Fe_2O_3	SiO_2, MgO, Al_2O_3, and inorganic oxides	SiO_2, Na_2O, Al_2O_3, K_2O and other inorganic oxides	NaMMT SBA 15, cloisite, bentonite, attapulgite, kaolinite, natural clay, hyper clay, smectite, kaolins, silicates, etc.	[30–32]
Morphological structure	Nano-tubes	Numerous shapes	Layered structures	Porous structures		[33,34]
Size of particle	Length of 0.5 to 2.0 μm; width 50–200 nm; pore size of 5–30 nm	Length of 5 to 100 μm; pore size of 0.1 to 1.0 μm	Length of 5 to 20 μm, thickness of separate layers: 0.7 to 2.5 nm	Length of few microns, and pore size of 0.5 to 2.0 nm		
Specific surface area (m^2/g)	20 to 150	16 to 70	10 to 200	100 to 900		[35–37]

an alkaline solution (e.g., NaOH, KOH, etc.). After completion of the chemical co-precipitation reaction, thermal treatment (30–100 °C) is performed in order to achieve the maximum yield of clay with excellent crystalline properties. Instead of thermal treatment at low temperature, a high-temperature hydrothermal method can be employed via heating the sample in an autoclave under high pressure (10–150 MPa) and high temperature (200–1000 °C) for a period of a few hours to days.

The ion exchange (indirect process) is also often employed for the synthesis of clays, and has been used for the intercalation of numerous types of anions. In an ion exchange process, LDHs are initially prepared with host common anions (e.g. NO^{3-}, Br^{-}, SO_4^{2-}, CO^{3-}, etc.), and then the anions present in the interlayers are exchanged with the direct anions. The host–guest exchange process is primarily dependent on the electrostatic forces between the positively charged clay layers and the exchanging anions. The anions are intercalated through two pathways: (i) de-intercalation of univalent anions (e.g., NO^{3-}, Br^{-}), which involve weak electrostatic intercalation with the layers, and (ii) strong interaction between the positive layers and anions, which can be easily exchanged with the univalent anions.

In another approach, the hydrothermal reaction proceeds with the inorganic metals either in the form of hydroxides or in the form of salts, or mixing of the selected anions in the desired pH conditions. The optimized pH values for very fine nanoscale Mg/Al-based LDHs clays and Zn/Al-based LDHs clays are 9–10, and 7–7.5, respectively. After optimizing the pH value of the reaction solution, it is transferred into a stainless-steel autoclave, is subjected to high pressure and temperatures from 50 to 180 °C, and the morphological, structural, and physico-chemical properties of the clays are controlled by hydrothermal process conditions such as reaction time, temperature, pressure, contact time, etc.

2.8. Applications of clays

Owing to their fascinating physico-chemical properties, clays are 2D-layer-structured inorganic materials that applied for various fields such as environmental remediation, in which they serve as potential materials for the removal of hazardous chemicals (e.g., radioactive U^{6+}, As^{3+}, Cu^{2+}, Cr^{3+}, phenols, dyes, etc.) from contaminated water or toxic gases (e.g., NO_x, soot released by vehicles) from the atmosphere, oxidation of alcohols and pure water for efficient production of oxygen, as alternative and new disinfectants in water treatment plants for killing of bacteria (E. Coli) by breaking down cell walls, as novel green antibacterial agents without producing any byproducts, and so on [38–49]. However, clays have limitations due to the presence of cracks and damaged areas, which deteriorate their properties. In the following sections, we discuss about the chemical methodologies for the development for developing self-healable polymers used to heal the cracks, as well as the properties of clays before and after healing.

3. Chemistry of self-healing materials (design and synthesis methodologies)

In order to protect or repair damaged or physically cut samples, the design and development of polymeric materials with self-healing or self-repairing characteristics have been recommended. These self-healing polymers are special class of smart materials, which can heal the internal defects/cracks or damage generated in any matrix and can rebuild the mechanical properties (e.g., tensile strength) of the cracked part through an autonomic healing process, as similar to the human skin when it is wounded. The fundamental concept of self-repairing mechanism of polymer requires understanding and designing of efficient polymerization reactions. Different methodologies were developed to impart self-healing characteristics to synthetic polymers.

3.1. Intercalation strategies of polymers in the interlayer galleries of clays

Various polymeric materials have been encapsulated inside the layers of different types of clay minerals through polymerization, solid-state intercalation process without using organic solvents, or intercalation through a long-term stirring of reaction suspension containing the clay and organic polymer. Gao et al. [50] reported intercalative polymerization of methacrylic acid (guest polymer) inside the interlayer galleries of Zn–Al-LDHs clays (host molecule) to fabricate PMA/LDHs material, in which PMA interacts with LDHs through hydrogen bonds, and utilized the material for the testing of environmental humidity. Polymethylene blue was intercalated inside nanofibrous-structured attapulgite clay mineral through electro-polymerization and the influence of reaction parameters on catalytic and electroactive characteristics of the material was investigated, as well as its sensing biomolecules through cyclovoltametic studies [51]. Polyaniline intercalated nanostructured attapulgite composites with excellent electrochemical properties were synthesized by *in-situ* chemical oxidative polymerization for developing an iodate sensor through cyclic voltametric and amperometric measurements [52]. Long-chain crown-ethers, non-ionic surfactants, ethylene and its derivative polymers were intercalated between the layers of dried vermiculites, montmorillonite, kaolinite, and smectite sheet clay minerals [53–55].

The expandable 2:1 swelling-type clays (e.g., smectite group) contain only siloxane surface reactive groups, whereas 1:1-type clays (e.g., kaolinite group) consist of two types of surfaces such as siloxane and hydroxyl (OH) surface reactive groups. The grafting of molecules (e.g., organosilanes, APTES, chloropropyltriethoxysilane) onto kaolinite clay minerals is difficult owing to hydrogen bond formation between the layers. To obtain a successful interlayer chemical grafting, a pre-intercalation process with small polar organic solvents such as dimethylformamide or dimethyl sulfoxide are used to fabricate an intercalate-precursor, and utilized as the substrate for an intercalation of organosilane [56,57]. Solid-state NMR studies were used to analyze both the molecular structure and dynamic behavior of organo clays and their chemically modified hybrid materials, the intermolecular interaction, and the structural organization through chemical shifts of the elements connected by chemical bonds [58,59]. Smectite sheet clay minerals were chemically grafted with amino- and mercapto-containing organosilanes, and the pristine smectite and chemically grafted smectite clays were investigated for the adsorption of heavy metal ions (e.g. Hg^{2+}, Pb^{2+}, and Cd^{2+}) from the contaminated water through an ion-exchange mechanism, in which the inner layer cations of smectite clay is replaced with heavy metal ions [60]. The same materials were chemically and covalently grafted with organosilanes (e.g., APTES, MPTMS) on their surface and studied as electrochemical sensors and biosensors for the detection of ascorbic acid and uric acid [60,61]. Bayraktepe et al. [62] reported a simple method for the fabrication of sepiolite clay mineral-modified carbon nanotubes and utilized it to identify an anti-cancer agent, shikonin content in biological samples through CV and differential pulse voltammetry (DPV).

The nanoplatelet-structured natural bentonite clay mineral was modified with polyhydroxo metallic citations through nanofillering process, and studied for oxidation of the 4-chlorophenol chemical pollutant in an acidic solution through such as electrochemical impedance spectroscopy (EIS), CV, DPV, and square-wave voltammetry [63]. The bentonite-modified material exhibits excellent electrocatalytic activity for nitride oxidation, and was used for the analysis of nitrite pollutant in clean water [64]. Tiwari et al. [65] developed hexadecyl trimethyl ammonium bromide (HDMA)-modified bentonite clay for low-level sensing of total arsenic (As^{3+}) content present in aqueous solution under different pH conditions from 2.0 to 10.0.

Sharma et al. [66] reported gelation modified-lap clay for the detection of urea. Wen et al. [67] developed rod-like palygorskite clay mineral-modified nanostructured carbon (graphene) material as voltametric sensor for simultaneous detection of xanthine (XA), hypoxanthine (HX) and uric acid (UA) in biological samples, which are important in the metabolism of organisms for the early diagnosis of human disease. Santos et al. [68] grafted N-isopropyl acrylamide (NIPAM) by using ammonium persulfate as the initiator, and used it as a temperature-sensitive material with the ability to switch from stiff to soft or from brittle to tough in response to slightly changing conditions such as temperature, pH, or electromagnetic field.

3.2. Self-healing strategies of polymers and its mechanism

The self-healable polymers have attracted much interest in the last few years. The self-healable characteristics of polymers give them the ability to self-heal cracked/damaged parts of materials, which would extend the durability and life span of many materials, reduce wastage, and enhance performance while utilizing them for practical applications in various fields such as construction, automobile, aerospace, defense, and biomedical engineering. Considerable development has been recently done in the designing and developing of novel self-healing polymers by various chemical methodologies. These polymers have the capacity to spontaneously repair cracks and damage under mild conditions that are desired in many applications.

The self-healing polymers can be categorized into intrinsic and extrinsic materials. In the case of extrinsic systems, external healing agents such as crosslinkers, organic monomers, or their liquid-like reaction mixture are used as encapsulating materials applied to the destroyed/cracked/scratched part, and repair the damaged parts of materials [69,70]. Interestingly, a 3.5-cm-long cracked part in the material was repaired, restoring the robust structural stability and mechanical behavior, by filling the liquid healing agent into damaged sites through an extrinsic healing route, which was followed by polymerization reactions [70]. Further, an intrinsic self-healing process occurs in the damaged material through intra or intermolecular forces such as strong chemical covalent linkage bonds, chemical/physical crosslinking networks, supramolecular interactions, coordination, and hydrogen bonds [71,72].

In some cases, the phase separation process in polymers can stimulate the self-healing process [73]. Polymeric materials are promising candidates for the self-healing applications, owing to their dynamic long-chain and complex chemical structure, and

the self-healing activity can be introduced to polymers through designed chemistries, or exposing them to chemical, physical, or thermal conditions. The high chain mobility of a polymer and its glass transition temperature (T_g) also determines healing efficiency. The healing efficiency of a material is normally estimated as the toughness ratio between the pristine sample and the healed sample. The self-healing process of various polymeric materials can be obtained through different strategies. Explanations of these strategies and mechanisms are provided below.

3.2.1. Photo-irradiation-assisted self-healing

Cheng et al. [74] reported photo-irradiation process for self-healing using resins. In this process, cracked films of crosslinked polyurethanes were synthesized on glass substrates by reacting 1,3-bis(eugenyl) glycerol diether and 1,6-hexanediisocyanate (HDI). The self-healing behavior of the polymer films was tested using ultraviolet (UV) irradiation. It was found that the cracked part of the polymer film was self-healed within 5 min, as shown in Fig. 3, indicating that synthesized polyurethanes show good self-healing properties under UV light, as well as high temperature resistance behavior (Td = 1000 °C). Thermogravimetric analysis showed 2.5% weight loss at 800 °C, indicating it exhibits excellent thermal properties owing to the presence of sulfur, aryl rings, and carbamates in the polymer chain. Another research group [75] fabricated crosslinked polyurethanes with disulfide reactive group in the main chain that displayed self-healing and re-structuring characteristics under solar irradiation. Such reactive groups (C–S or S–S) in the polymer chain can be easily synthesized, and they lead to self-healing under photo-irradiation or thermal treatment.

Arslan et al. [76] applied S–S bond cleavage-reformation reaction and supramolecular interactions to develop self-healing property. In this process, they prepared a low-cost and self-healable poly(benzoxazine-*co*-sulfide) through the inverse vulcanization reaction between poly(propylene oxide)benzoxazine, diallylbenzoxazine, and different contents of elemental sulfur at 185 °C for 30 min, and tested its self-healing performance and fracture toughness. It was found that crosslinked polymer films could successfully heal themselves five times, and healed specimens showed good fracture toughness properties ($\eta = 30$) owing to simultaneous ring opening polymerization reaction of benzoxazines and inverse vulcanization between elemental sulfur and allyl reactive groups.

The self-repairing can occur in intrinsically healing systems through external stimulants such as high temperature and light irradiation ($\lambda > 300$ nm). For instance, light-driven healing systems include coumarins, where light-stimulated reversible chemical reactions take place through cycloaddition of coumarin and cinamoyl reactive groups; and the cycloaddition reaction of anthracene and their derivatives [77], and the modification of suitable polymers with these coumarin derivatives by side-chain or main-chain, lead to self-healing activity through photo-induced cycloaddition reaction mechanism, or grafting of photosensitive moieties on the polymer chains. Such derivatives are attached to various synthetic polymers such as polyurethanes, polyoxazolines, and PEGs [78,79], and the healing ability is dependent on applied wavelength.

Zhao et al. [80] employed a single-step route for the synthesis of photo-healable polymers from the reaction of epoxidized oil by the photo-initiated thiol-epoxy addition reaction in the presence of UV irradiation. Here, epoxidized oil acts as the main raw material and 7-mercapto-4-methyl coumarin act as the photo-healing reactant (known for its dimerization) that graft onto epoxidized triglycerides through its SH-groups. Therefore, thiol-epoxy addition reaction and dimerization of coumarin reactive groups are expected under UV light to generate photo-crosslinked and photo-healable polymer (Fig. 4). Self-healability of the developed polymer film was determined by pendulum hardness measurement, from which the Konig hardness was calculated after each irradiation stage as a function of the irradiation cycle number. It was observed that hardness of polymer film decreased after irradiation at $\lambda = 255$ nm owing to photocleavage of the grafting coumarin derivative into the grafted monomer. Then, the hardness of film can be regained after irradiation at $300 < \lambda < 450$ nm, which confirms photo-reversible reaction.

Kiskan et al. [81] reported a novel self-healing strategy for the four types of photo-healable poly(propylene oxide)s containing coumarine–benzoxazine units (PPO-Coum-Benz)s through a photo-induced coumarine dimerization reaction. The crosslinked polymeric films are prepared by a solvent casting of different compositions of (PPO-Coum-Benz)s in chloroform on the surface of Teflon sheets, followed by thermal ring-opening reaction of benzoxazine active groups at 210–240 °C. It was found that photo-healing and toughness of polymer films were enhanced after irradiation by UV light $\lambda = 300$–350 nm). The healing efficiency (η) for the cracked sample was 44%, and for damaged sample was 10%, demonstrating that cracked specimen exhibited better healing efficiency owing to efficient dimerization of coumarine groups under UV irradiation.

3.2.2. Microcapsule-based self-healing process

The self-healing ability of polymers can be obtained in two ways. In autonomous self-healing processes, the polymer is encapsulated with small microcapsules that contain the healing agent that is released into the polymer when the capsule shell is damaged. This technique is known as the microcapsule-based self-healing process. In contrast, stimuli-assisted healing processes need an external stimulus (e.g., light, redox reaction, pH, thermal heating, assistance of liquid monomer, catalyst, additives or solvents) to activate the healing reaction that involves breaking of bonds and bond reconstructing process [82,83].

Epoxy-based healing polymers were developed using cyclopentadiene as a healing agent and Grubb catalyst through microcapsule-encapsulated self-healing technique [84]. This healing technique is good only for thermosetting polymers (e.g., epoxy, PF, MF) as the connection between the liquid healing agent and previously crosslinked thermoset is not efficient. The main drawback of capsule-based method is that it can heal the polymer surface only one time, but reversible breaking and rebuilding of the chemical bond-based healing method can achieve a healing reaction that offers a recyclable healing process.

3.2.3. Self-healing through reversible bond formation

Intrinsic strong and fast-healable polymers have great importance owing to their capacity to freely repair mechanical damage (thick cracks or surface scratches) multiple times. There has been a challenge to synthesize such polymers to obtain both healing efficiency (complete recovery) and mechanical strength that is comparable to that of conventional non-self-healing polymers of same group. Efforts were made to synthesize a novel class of polymers with excellent healing efficiency through reversible non-covalent bonds or reversible-covalent linkages [85,86]. Such polymer systems based on reversible supramolecular interactions (e.g., several hydrogen bonds, weak van der Walls interactions via side branches, or metal–ligand coordination complex) can display high healing capacity at room temperature, as well as mechanical behavior that is similar to conventional polymers under short-time quasi-static loading conditions [87,88]. However, these types of self-healing polymers have weak mechanical strength owing to their temperature-dependent nature, and the dynamic nature of reversible chemical bonds. Therefore, different polymers prepared based on strong covalent bonds (e.g., acylhydrazone bonds, boric ester bonds, sulfide bonds, Diels–Alder (DA)

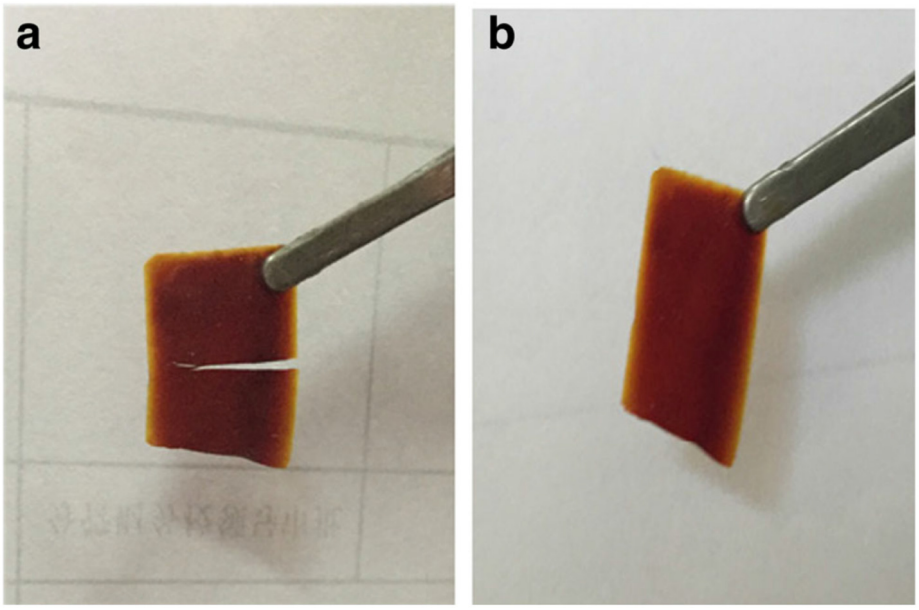

Fig. 3. Self-healing polyurethane films: (a) damaged part of film, and (b) self-healed polymer film after UV irradiation process [74].

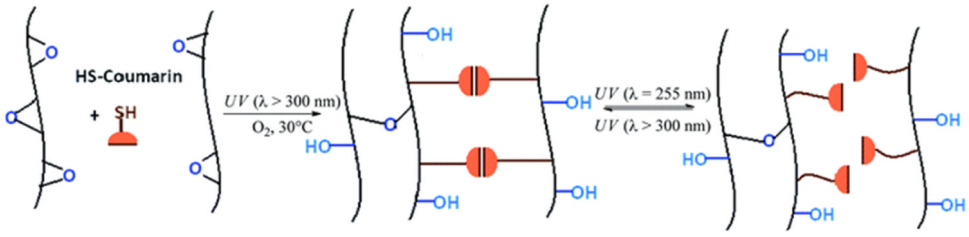

Fig. 4. Preparation of photo-induced self-healing polymer under UV and air through photo-initiated thiol-epoxy chemistry.
Source: Reprinted with permission from Ref. [80].

reaction) provide superior mechanical behavior in a wide range of temperatures owing to greater stability of the reversible bond moiety [89–91]. However, they exhibit lower healing properties.

Garcia et al. [92] studied the effect of polymer architecture on the healing process and its kinetics. Different strategies have been developed to achieve polymers with high healing capacity and enhanced mechanical stability. The crosslinked aromatic disulfide-based poly(urea-urethane) heals at the room temperature without involving a catalyst [93]. Such crosslinked polymer-bearing disulfide bonds that are linked to aromatic rings are re-processed after curing reaction at high-temperature and pressure, resulting polymer films with new structure without losing their mechanical stability [94], and their self-healing activity occurred via H-bonds and aromatic disulfide bonds. Grande et al. [95] described the synthesis of a series of poly(urea-urethane) with different crosslinking densities and the same number of dynamic covalent linkages (S–S bonds) through different combinations of fixed a disulfide content, trifunctional polyurethane, and bi-functional polyurethane pre-polymers (linear PU4000 and three-armed PU6000). They investigated the effect of polymer structure and the number of reversible reactive groups on macroscopic healing nature and mechanical properties of the synthesized polymers. The healing kinetics and healing efficiencies were measured as a function of network composition, contact time, and temperature. Dynamic mechanical thermal analysis, tensile (ISO 527 A standard), and fracture studies were conducted to determine the degree of mechanical strength recovery of samples after damage at room temperature. The time–temperature protocol was used for both the rheological and fracture studies, indicating the relation between the processes for macroscopic healing and polymer architecture.

Wang et al. [96] developed transparent and healable polymers with excellent multifunctional properties of mechanical strength, elasticity, resilience, and healability by complexing poly(acrylic acid) (Mw ca. 450000) and poly(ethylene oxide)s with different molecular weights (Mw ca. 100000, 300000, and 600000) via the hydrogen-bonding interactions (Fig. 5a to d). Such polymers showed good mechanical properties (real strength at break) of 61 MPa and toughness (fracture energy) of 22.9 kJ/m^2, with elasticity to over 35 times to their initial length. Interestingly, they also found that polymers have ability to return to their original length after removal of applied stress, and the ability to heal from damage or physically cutting of samples in a humid environment. This is due to restructuring of reversible hydrogen bonds between the two polymers; such chemical bonds serve as crosslinkages. Furthermore, a water-enabled healing property was established by the dispersion of ultrasmall silver nanowires on the surface of polymers (Fig. 5e). This methodology is anticipated to be useful to synthesize a wide range of other polymeric materials for developing efficient healable systems.

Yang et al. [97] employed reversible bonds concept for the synthesis of a tough self-healing disulfide-containing poly(urea-urethane) that has excellent mechanical strength and self-healing efficiency (Fig. 6) as well as the ability to repair itself a number of times. It was found that two pieces of cut samples were healed and the healed sample has a healing efficiency of 75.3%; the efficiency increased to 97.4% with increasing healing time, with

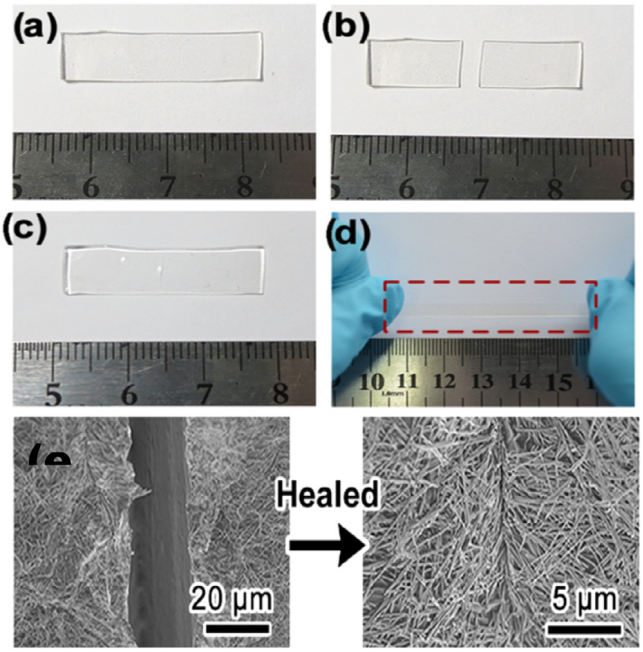

Fig. 5. Photographs of PAA-PEO copolymer sheet before (a) and after (b) being cut into two sheets, (c) healed sample of (b) after one hour, (d) stretched sample of (c) to 175% strain, (e) FE-SEM image of Ag nanowire-coated polymer sample after being cut and healed.
Source: Reprinted with permission from Ref. [96].

tensile strength of 7.5 MPa owing to a sufficient number of S–S bonds in the polymer chain.

Xiao et al. [98] developed intrinsic self-healing waterborne polyurethanes (Fig. 7) by increasing the number of hydrogen bonds or inducing reversible crosslinks to the polymer that contain sulphonate reactive groups, which were initially synthesized from poly(tetramethylene glycol), poly(1,4-butylene adipate glycol), and isophorone diisocyanate. It was found that with increasing of soft content in polyurethanes, the healing efficiency was increased at 100 °C for 18 h (Fig. 8). Another group investigated the fracture healing and rheological behavior of two different poly(urea-urethane)s that consist of (i) hydrogen bonds and (ii) both hydrogen bonds and disulfide linkages [99]. They found that each reversible bond in the polymer matrix played an important role in the enhancement of the network behavior (rheology) and healing (fracture). The reversible bond concept was also employed to synthesize poly(methyl triethylene glycol acrylate)-cyclodextrin (CDs) that exhibit stretching and self-healing properties [100].

Martin et al. [101] used thiolate exchange, aromatic disulfide exchange, and thiolate/disulfide exchange) as a new strategy to develop self-healing poly(urea-urethane), in which reversible bonds can be utilized to generate soft systems that can self-mend under ambient conditions. These polymers showed remarkable self-healing and elastic properties, as shown in Fig. 9. Likewise, various strategies have been employed to design and develop different novel synthetic polymers with high self-healing efficiency [102–108].

3.2.4. Controlled/living polymerization-driven self-healing

The living polymerization process involves the chain transfer and chain termination are absent. In many cases, the rate of chain initiation is faster than that of chain propagation, such that the number of kinetic-chain carriers is constant throughout the polymerization process. Various polymers with narrow molecular weight distribution have been synthesized via this technique, and this special property plays key role in various applications in numerous fields [109–112].

The living polymerization follows anionic, cationic, and radical polymerization. The most popular one reversible addition-fragmentation chain transfer (RAFT) and atom transfer radical polymerization (ATRP) are good examples of living radical polymerization [113–117]. This method allows the precise synthesis of polymers, organo–inorganic hybrids, or block copolymers (from low-cost monomers) with well controlled molecular weight, narrow molecular weight distribution, first-order kinetic behavior, site-specific functionality with high reactivity, diverse physico-chemical properties, long-lived polymer chain with preserved active end functional groups that resume polymerization reaction with another monomer, and complex polymer architectures such as comb structure or star morphology [118–121].

In the ATRP technique, the chain transfer and chain terminations are absent, and it consists of living chain end that again initiates the polymerization reaction with available reactive monomer. The block copolymers can be synthesized through this technique as the polymer is synthesized in various stages, in which each stage relates to a different monomer. Therefore, the monomer embedded in the living block copolymer matrix has a strong ability to repair the formation of cracks in the structural materials at ambient temperature through the formation of efficient covalent linkages, which rebuild the mechanical properties of the polymer. The healing efficiency of this type of polymer can be further improved by increasing the number of functionalities in the block copolymer.

Banerjee et al. [122] demonstrated a facile route to develop fluorescence-activated self-healable polymers by incorporating fluorescence-responsive ionic block copolymers (IBCPs) that are synthesized through combined methods of ring-opening polymerization (ROP) of ε-caprolactone, and xanthate-intermediated reversible addition-fragmentation chain transfer (RAFT) polymerization reactions. In this process, polycaprolactone was functionalized with xanthate to develop a PCL-based macro-RAFT active agent utilized to synthesize block copolymers with cationic poly (2-(methcryloyloxy)ethyltrimethyl ammonium chloride) (PCL-*b*-PMTAC) and anionic poly(sodium-4-vinylbenzenesulfonate) (PCL-*b*-PSS). During the block copolymer formation, cationic segments

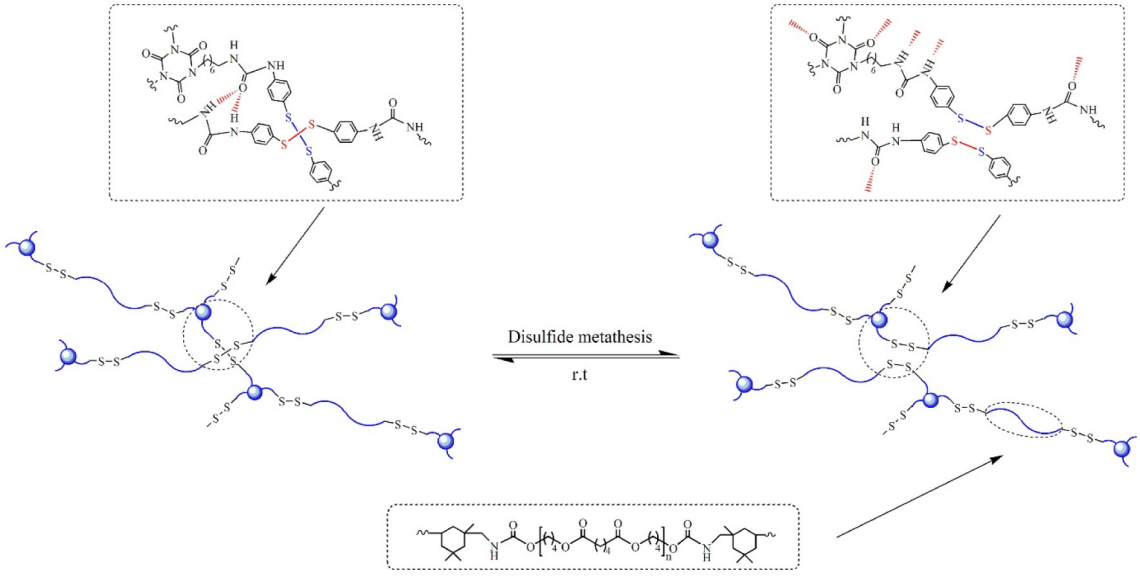

Fig. 6. Healing mechanism of a disulfide-containing poly(urea-urethane).
Source: Reprinted with permission from Ref. [97].

are copolymerized randomly with a trace amount of fluorescein O-acrylate as an acceptor, whereas the anionic segments are randomly copolymerized with a trace amount of methyl methacrylate-based donor to make both the segments fluorescent. The positively charged IBCPs are encapsulated into polyacrylamide that showed excellent properties of both self-healing and fluorescent. They also found that mechanical properties of the healed polymer were similar to those of the uncut polymer sample. The healed polymer displayed 550% elongation, whereas the uncut polymer showed 700% elongation before breaking owing to the creation of stretching ionic interactions between the two segments in the polymer chain.

Pramanik et al. [123] using RAFT technique developed a novel class of self-healing ABA tri-block copolymer poly(furfuryl methacrylate-*b*-poly(dimethyl siloxane)-*b*-poly(furfuryl methacrylate) (PFMA-*b*-PDMS-*b*-PFMA) in the presence of PDMS-CTA as the macro-RAFT active agent. In this tri-block copolymer, a DA click reaction was conducted between the reactive furfuryl group in PFMA unit as the diene with different maleimides as the dienophile. PFMA unit in the ABA BCP makes the copolymer thermally stable, whereas PDMS makes it suitable as hydrophobic self-healing agents. The self-healing property of BCP was investigated by DSC and SEM. The polymer (FDF/BM DA) films were fabricated on the glass surface and notches were made on the film surface with a thin blade; the healing of the cut part of the film was studied at different temperatures and time intervals using electron microscopy. Healing-efficiency of the synthesized DA polymer was studied by optical surface profilometry using a 3D optical microscope, for which the sample was prepared on a glass slide by the drop-casting method. After the rDA reaction at 150 °C, and subsequent heating at 50 °C for 14 h, SEM images showed that scratches and fractures were healed completely, and the samples showed repeatable healing owing to DA and rDA reactions. They also noticed that the healed DA polymer revealed the hardness of 0.28 GPa with the contact depth of 39.92 nm, which was almost similar to the pristine DA polymer.

Dohler et al. [124] employed combined click chemistry and living carbocationic polymerization to develop crosslinking hyperbranched azide- and alkyne-modified poly(isobutylene)s with the molecular weight (Mn) of ∼30000 g/mol (with active end groups), which act as room temperature self-healing polymers without external stimuli such as UV-irradiation and thermal heating. This click-based reaction is a faster, efficient catalytic process, and leading to a polymer with effective crosslinking. Moreover, the number of end groups of polymer increased crosslinking densities and reduces gelation times during network formation. Several crosslinking strategies were established based on catalytic reactions such as ROMP, epoxy crosslinking, siloxane- and thiol-malemide healing materials [125–129]. Long et al. [130–133] employed combined esterification and ring-opening polymerization to synthesize amphiphilic polymers with desired properties such as uniform size and morphology, low toxicity, luminescence and biocompatibility. They also employed other strategies such as supramolecular chemistry, multicomponent reactions (MCR), and emulsion polymerization to fabricate different polymers with desired characteristics [134–140].

Herbst et al. [141] employed the combined living carbocationic polymerization and azide–alkyne "click" reactions to study self-healing properties mono- and bi-functionalized supramolecular poly(isobutylene)s (PIBs) with hydrogen-bonding moieties. They found that these hydrogen-bonded PIBs shows self-healing behavior at room temperature after being cut into two half-disks and brought into physical contact at the fractured surfaces. The living anionic polymerization [142] was used to develop well-defined poly(furfuryl glycidyl ether) (PFGE) homopolymers and poly(ethylene oxide)-*b*-poly(furfuryl glycidyl ether) (PEO-*b*-PFGE) block copolymers with self-healing properties and studied by DSC, profilometry, and depth-sensing indentation. The results revealed that block copolymer films had strong ability to heal complex scratches multiple times.

Barthel et al. [142] used the living anionic polymerization approach to develop well-designed block copolymers of poly(ethylene oxide)-*b*-poly(furfuryl glycidyl ether) (PEO-*b*-PFGE) as the self-healing materials. These polymers were obtained by the formation of thermo-reversible bonds within drop-cast polymeric sheets through rDA reaction between furan reactive groups in the side-chain of PFGE segments and a bifunctional maleimide that acts as a crosslinking agent. The self-healing properties of these block copolymers were analyzed via depth sensing indentation, profilometry, and DSC, and the results showed that the polymers are capable of healing scratches (1.7 μM depth, 0.22 mm width, and 3.5 mm length) in the polymer films over multiple cycles. After crosslinking, these block copolymer films showed a

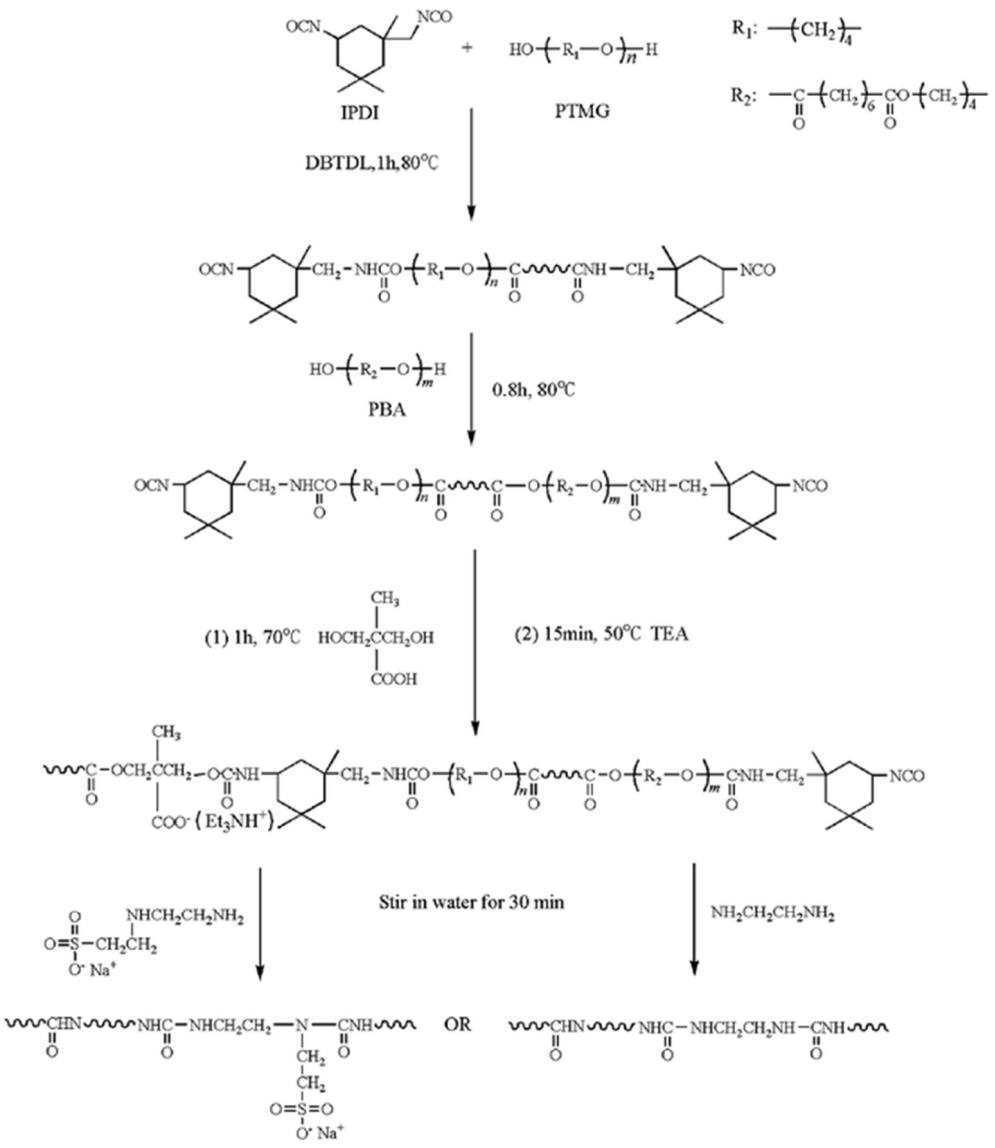

Fig. 7. Synthesis process for self-healing waterborne polyurethanes. Reprinted with permission from Ref. [98].

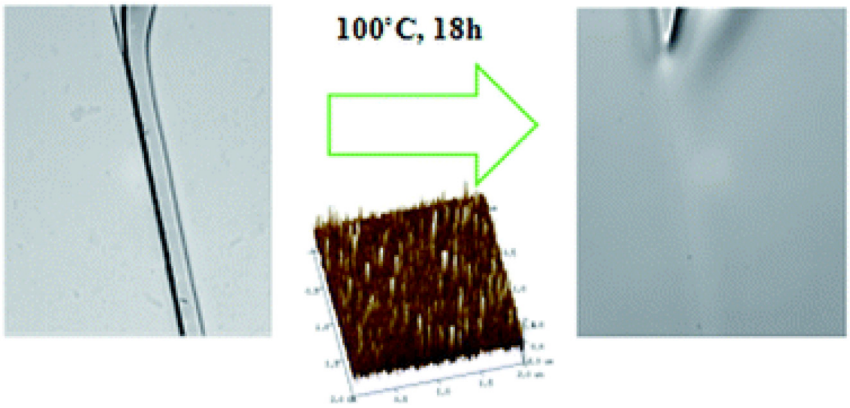

Fig. 8. Optical images of synthesized polyurethane before and after healing at 100 °C for 18 h.
Source: Reprinted with permission from Ref. [98].

hardness of 0.6 GPa and a stiffness of 5.13 GPa, demonstrating their visco-elastic properties.

Other novel self-healable polymers [143] such as PMMA-based material was synthesized with encapsulating glycidyl methacrylate (GMA)-modified poly(melamine-formaldehyde) through an

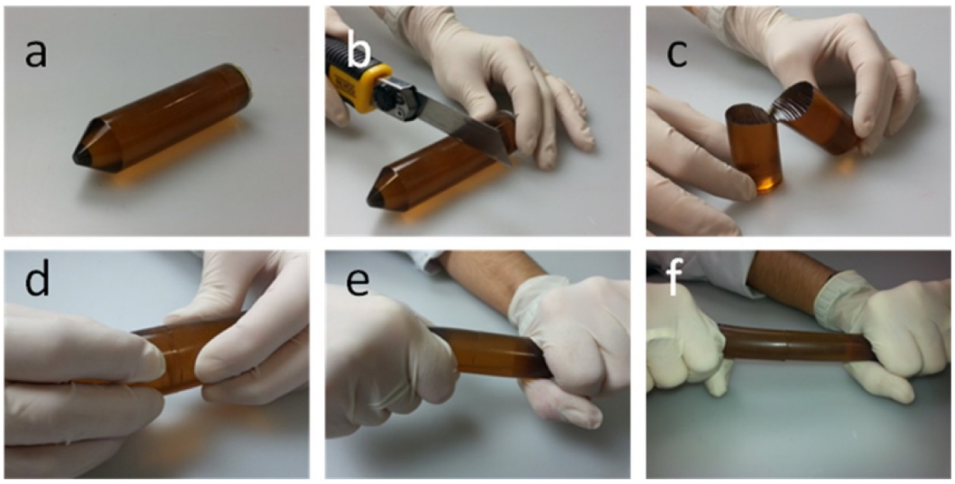

Fig. 9. Photographs of cylindrical disulfide-crosslinked poly(urea-urethane) (a), which was cut in two pieces (b, c), two pieces are permitted to combine for two hours through simple surface contact (d), formation of self-healed polymer (e), and stretched sample after healing (f).
Source: Reprinted with permission from Ref. [101].

ATRP reaction using two different types of initiating agents (linear and hexafunctional types). GMA is a low-viscosity organic monomer and used as a core material that easily undergoes a copolymerization reaction with living PMMA prepared by fast and controlled polymerization at room temperature through the ATRP technique. These linear and six-armed star PMMA have active living groups that initiate the healing process covalently by encapsulating the monomer to the areas of cracks. Field-emission scanning electron microscopy (FE-SEM) images of polymers are shown in Fig. 10(a and b) before and after the healing process. The healing-efficiency of two different polymers as a function of time is shown in Fig. 10c. Both polymers regained 100% of their original fracture toughness after the healing reaction.

Liu et al. [144] employed RAFT and click chemistry to develop low-cost lignin-*graft*-poly(5-acetylaminopentyl acrylate) (lignin-*g*-PAA) (Fig. 11) with self-healing characteristics (Fig. 12). Here, a copper-catalyzed azide–alkyne cycloaddition reaction or "click" reaction is utilized to strongly connect the lignin and an end-group-functionalized PAA. Lignin-*g*-PAA showed a well-defined nanostructure and rubber-like viscoelastic flexible properties owing to the formation of a high rate of hydrogen bonds from the acetylamino groups. Another novel self-healable poly(dimethylsiloxane) crosslinked with coordination complexes was synthesized with multifunctional properties such as autonomous self-healing behavior at −20 °C, high flexibility, excellent dielectric strength, and mechanical actuation [145].

3.2.5. Crack healing via molecular interdiffusion approach

Molecular interdiffusion is used for healing cracks. This technique occurs at healing temperatures (T) higher than that of glass transition temperature of the polymer (T_g), which is diffusion of polymeric chain segments across the interface [73]. With increasing healing time (t), the interface strength also increased, which reached maximum value after healing of the complete interface. The healing properties are faster at higher temperature owing to improved intermolecular diffusion of dangling chain at the interface. Both single cracks, and mechanically occurred fracture/damage (microvoids) are healed completely by the chain intermolecular diffusion above the T_g value of different polymers.

In hydrogels, the dangling chains, which are chain segments, one end of which is not attached to the network, are responsible for repairing the crack, because the dangling chains display segmental interdiffusion, similar to liquid [146]. Boiko et al. [147] investigated the molecular mechanism of self-healing on glassy (amorphous) polymers such as poly(2,6-dimethyl-1-4-phenylene oxide), polystyrene, and PMMA. The self-healing properties were tested by heating the polymer samples for the fixed period. When, pieces of the same polymeric material were permitted to contact at above the T_g values, the interface slowly vanished and mechanical properties at the interface between two polymer sample pieces increased due to complete healing of cracks through molecular diffusion across the interface. The healing occurred above the T_g values in the range of −50 °C to + 100 °C.

3.2.6. Layer-by-layer (LBL) assembly-assisted crack healing

The LBL assembly approach has been used to repair damages (cracks or cuts) of materials in the presence of an aqueous solution [148]. Polyelectrolyte multilayer films fabricated via this method can stimulate from cuts or cracks of several tens of micrometers length and width in the presence of deionized water. The drawback of this technique is that the fabrication time is too long, which restricts the process for large-scale industrial applications. In order to overcome this issue, a spray-based LBL process has been introduced, in which polymer solutions are directly sprayed on the substrates [149,150]. Polyelectrolyte polymers used in LBL methods having repeating units that hold an electrolyte group (strong or weak). Strong polyelectrolyte films completely separate in the aqueous system owing to strong acid and base groups connected to the repeating units of the polymers. In contrast to this, with weak polymer electrolyte films (weak charge groups such as –COOH, $–NH_2$), the ionization completely depends on pH of the solution.

The automated spray-based LBL method was employed to fabricate poly(ethyleneimine)/poly(acrylic acid) multilayer films (PEI/PAA) on substrates and the effects of LBL parameters on the variations in roughness, thickness, and an elasticity of multilayers were studied. The healing phenomenon was observed in PEI/PAA films through the decrease in the polymer viscosity and interdiffusion of polyelectrolyte at the damaged zones in the aqueous environment [151]. Huang et al. [148] applied the spray-based LBL technique to fabricate BPEI-Ag NPs-PAA multilayer films (25 μm thickness) that heal scratches between 70 and 80 μm.

3.2.7. Polymer hydrogels for crack healing

Getachew et al. [152] fabricated hydrogels by *in-situ* chemical graft polymerization of 2-acrylamido-2-methyl-1-propanesulfonic acid (AMPS) on the surface of porous structured poly(ether sulfone) (PES) substrates, and successfully established self-healing

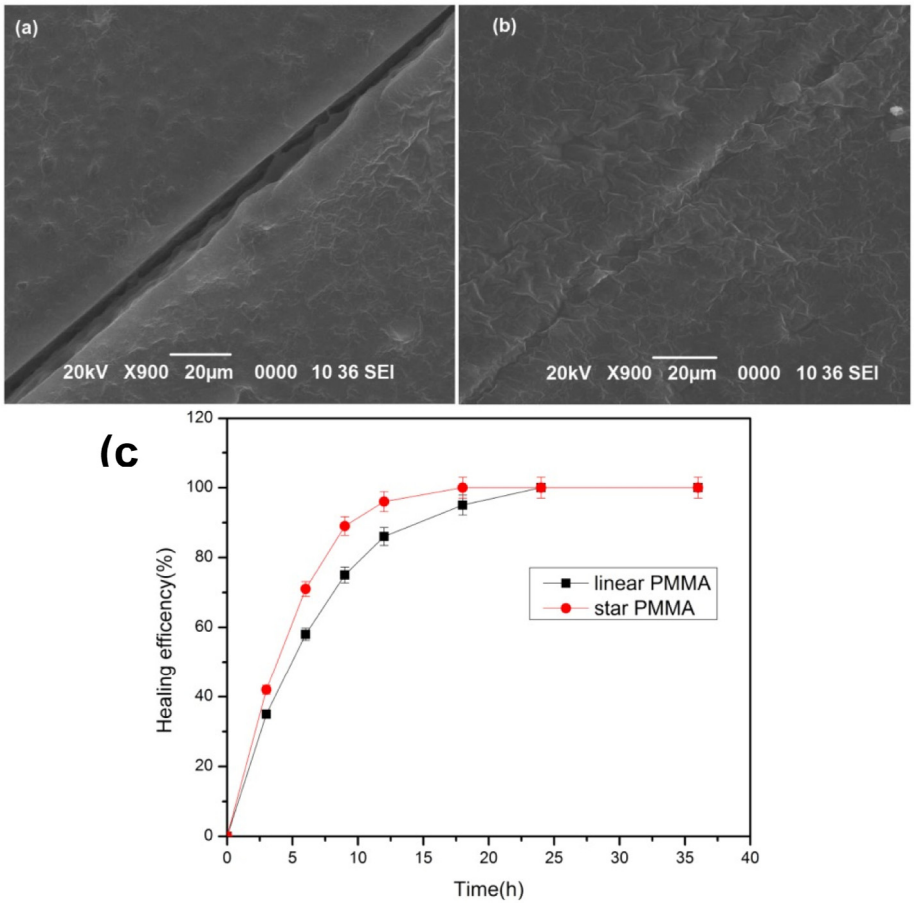

Fig. 10. Electron micrographs of pre-notched polymers before (a), after (b) healing process, and the healing efficiency of two types of polymers with time (c). *Source:* Reprinted with permission from Ref. [143].

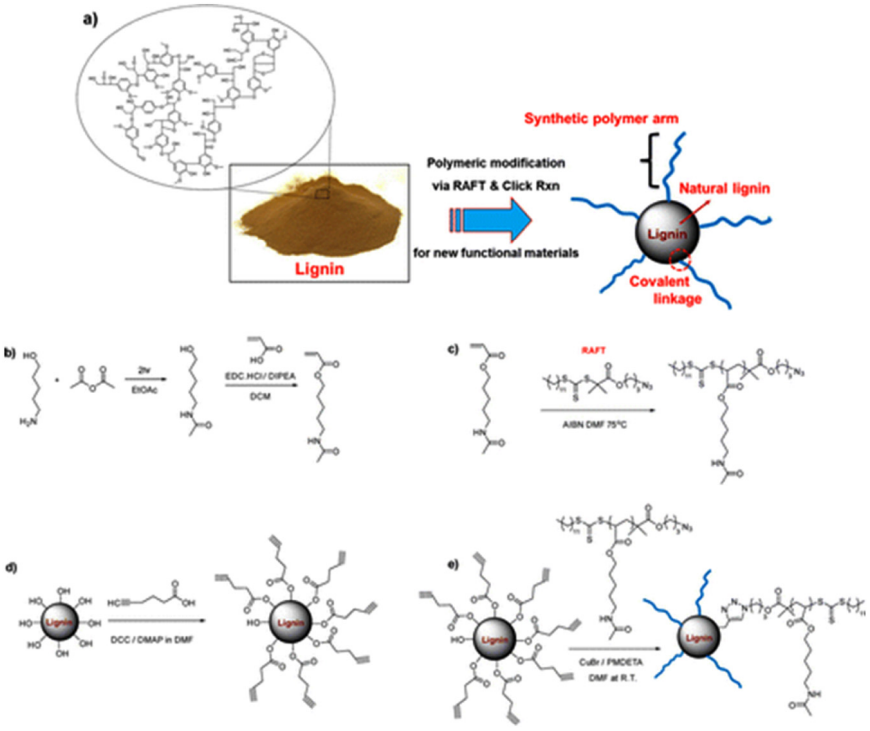

Fig. 11. Synthesis route for preparing self-healable lignin-*graft*-ply(5-acrytylaminopentyl acrylate). Reprinted with permission from Ref. [144].

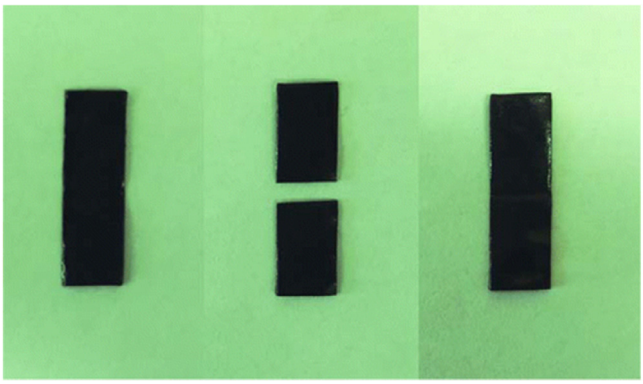

Fig. 12. The test of self-healing activity under ambient conditions (23 ° C and 55% humidity). The original undamaged lignin (20 wt%)-*graft*-PAA (left), material that cut into two half pieces (middle image), and the complete healing of material after connecting the two pieces at the interface.
Source: Reprinted with permission from Ref. [144].

properties owing to the presence of strong covalent linkages between hydrogel and the substrate. In this technique, hydrogels (hydrophilic polymers) enter into crack or damage site, absorb water and swell while maintaining the 3D structure, thereby resulting in self-healing in the damaged area through the swelling nature of the hydrogel, presence of H-bonds, and molecular interdiffusion [153–156]. The formation of hydrogen bonds can be the basis for self-healing, because those bonds freely reorganize after being broken. The molecular interdiffusion leads to self-healing property owing to the stochastic movement of macromolecular chains that leads to diffusion across the crack or fracture.

3.2.8. Recombination of chain ends-driven crack healing

The recombination of chain ends is another method introduced to heal damages or cracks in structural materials that have lost strength or have undergone molecular chain scission. In this technique, the active end groups present in the polymer play a key role in the recombination reaction and the healing process [157–160]. Barcan et al. [161] employed the reversible ring opening polymerization reaction to develop of cyclic carbonates containing pendant dithiolanes from PEO diols to create copolymers consisting of central PEO block and terminal dithiolane blocks. These polymers can be injected to damaged or cracked part through a syringe, and showed self-healing activity, as well as quickly regaining the mechanical strength after strain deformation. The healing-efficiency and other dynamic properties of these polymers can be tuned by controlling the number of dithiolane units, pH, and temperature. Other groups also employed this approach to synthesize self-healable crosslinked poly(n-butyl acrylate)-based polymers [107,162,163].

3.2.9. Nanostructured material-assisted self-healing

Nanoscale materials (size < 100 nm) have been proposed as a new and interesting approach to heal or repair cracks in materials that are mechanically damaged, either internally (crack) or externally (scratch). This method does not participate in the breaking or reconnecting of polymer chains, as other self-healing methodologies and healing mechanisms explained previously. Rather, these nanoparticles serve well as dispersants to fill the damage part and heal the cracks [164]. It was reported that the interfacial microcracks in composite materials can be detected and repaired using photothermal conversion inorganic nanoparticles [165]. In this process, Ag–Cu_2S nanoparticles were deposited on the surface of poly(*p*-phenylene benzobisoxazole) (PBO) through polydopamine chemistry, in which the nanoparticles undergo a photothermal effect that strongly converts the light energy into *in-situ* heat generation under xenon light irradiation. Then, a polyurethane matrix was used to prepare composites with PBO. They observed that the interfacial damage caused by a single fiber pull-out was easily self-healed in the presence of xenon light, leading to advanced hybrid materials with light-triggered self-healing characteristics.

Different micro- or nanoparticle-mediated photothermal approaches have been used for healing cracks, in which a small number of well-dispersed nanoparticles effectively absorb light, and convert the light to heat in the crack or damaged zone, resulting in new bonds (chemical covalent or physical) forming to generate self-healing or repairing in the crack area [165–168]. Likewise, various inorganic nanoparticles such as SiO_2, Fe_3O_4, MoS_2, $CaCO_3$, SWCNTs-Al_2O_3, Pt, Ag, organic carboxymethylcellulose (CMC) particles, and crosslinked polystyrene nanoparticles were used for fabricating various polymers with self-healing properties [148,169–177].

3.2.10. Mussel-inspired chemistry-assisted self-healing

Mussel-inspired chemistry has been used for the surface functionalization of materials and for the synthesis of self-healable materials with good healing performance such as high self-healing efficiency at room temperature and stronger mechanical
strength [178–181]. Mussels can strongly attach to a wide range of substrates with excellent binding strength, including wet surfaces-based substrates. Using efficient mussel-inspired chemistry, various polymers such as polydopamine, poly(4-vinylpyridine), polyethyleneimine, polydopamine–poly(N-acryloyl glycinamide), polydopamine-polyacrylamide (PDA-PAM), polyethylene polyamine, etc. have been developed [182–186]. Compared to other polymers, dopamine based polymers (polydopamine) have several advantages such as they can be easily coated on any type of organic and inorganic substrates, including on the surface of superhydrophobic substrates. Thickness and stability of polydopamine can be controlled on these substrates by changing parameters such as concentration of monomer, initiator, pH conditions, etc. Since polydopamine has several functional groups such as amino, carboxyl, phenolic, and imine, they can be easily disperse into various aqueous and organic solvents and leading to excellent hydrophilic property.

Combination of mussel-inspired chemistry and other polymerization methods (e.g. photoinduced electron transfer–atom transfer radical polymerization, Mannich reaction, MALI reaction, Kabachnik-Fields reaction, grafting from, grafting onto, surface initiated oxidative polymerization, etc.) have been used to develop multifunctional polymer hybrids with combination of various amine-based polymers and nanoparticles such as nanocarbons (e.g. graphene, porous carbon particles, CNTs, quantum dots, etc.), metal oxides, metal sulfides (MoS_2), noble metallic particles (e.g. Ag, Au, Pd, Pt, Au), MXenes, LDHs, transition metal ions

(e.g. Fe^{3+}, Mn^{2+}, Cu^{2+}, Ni^{2+}, etc.), and they can be potentially used in a wide range of applications across chemical, engineering, technology and biological and medical fields [187–198].

3.2.11. Schiff base reactions based self-healing

Schiff Base is also one of the efficient methods for the fabrication of self-healing polymers and for the surface modification of various substrates with excellent healing efficiency [199,200]. Schiff base is also known as "privileged ligand", and it is a synthesized ligand that formed by condensation reaction of aldehydes with imines and is utilized as efficient and reusable catalyst for various homogeneous and heterogeneous organic reactions. Ligand can form bonding strongly with transition metal ions and stabilize the oxidation state of metal ions in various conditions and leads to metal complex with high catalytic activity. Unlike other self-healing strategies requires external parameters such as temperature, light, pH, etc., Schiff base reactions are covalent type that can repair themselves without external parameters. When this ligand exposed to aqueous system, water molecules can promote the properties of Schiff base reactions. Schiff base reactions have been used to develop various self-healable polymers such as difunctionalized PEG, polydopamine/starch blend films, vanillin/chitosan hydrogel, polyurethane crosslinked with the Schiff base, gelatin-di benzaldehyde PEG, chitosan-modified PEG, amphiphilic poly(N,N-dimethylacrylamide-co-2-(benzylidene-hydrazonomethyl)-phenol) with Schiff based ligand, etc. [201–205].

4. Crack healing of clays and other inorganic solid materials using self-healing polymers

The cracks, cuts, damages, or defects present in the clays or soil clays are a critical issue in geotechnical engineering and infrastructure engineering. The cracks significantly affect the hydraulic and mechanical performance of dams, landfill liners, and land slopes [206]. The initiation, propagation, development, and network/patterning of cracks in the soil clays can significantly increase the hydraulic conductivity and enable water infiltration. Cracks can also form a slip surface that has no shear strength, resulting failure of slope. Therefore, it is necessary to develop new technologies to heal the cracks or damages present in clays.

Various strategies have been developed to heal or repair cracks present in different types of clays, concrete, and other inorganic materials such as ceramics, inorganic composites, and resin matrix composites. It was reported that concrete can slowly heal the cracks in the damaged area of materials through the presence of unhydrated cement particles or through the encapsulation of the healing agents or bacteria that generate limestone (calcium carbonate, $CaCO_3$) [85]. Silicon carbide (SiC) or whiskers were used at high temperature (>1000 °C) to fill the cracks with SiO_2 particles and heal the cracks present in ceramic materials [207]. In this process, SiC is converted into very small SiO_2 nanoparticles that fill the damaged areas and heal the cracks through high-temperature oxidation of SiC in the fractured environment. Other researchers [208,209] used similar strategy of microbially induced $CaCO_3$ precipitation (MICP) to enhance self-healing efficiency by inclusion of crosslinked acrylamide-based superabsorbent polymer and $CaCO_3$ into clays or other materials that have cracks.

De Camillis et al. [210] studied the effects of wet–dry cycles with natural seawater on the self-swelling capacity, swelling ability, crack formation, and hydraulic conductivity of two types of bentonites: pure bentonite and polymer (2 and 8%)-modified bentonite. They found that polymer-modified bentonite showed superior performance in the presence of electrolyte solutions. The two materials were exposed to six wet-dry cycles for the swell tests and four cycles for the hydraulic conductivity tests. The results from the 1D swell tests showed that the 8%-polymer-modified bentonite had good swelling properties and the thickness after six cycles was similar to the original thickness of unmodified bentonite. The polymer-modified bentonite showed low permeability to water during the wet–dry cycles ($\kappa = 9.11 \times 10^{-11}$ m/s), and the −CT scanning tests revealed that the modified clay had good self-healing ability and fewer cracks than the unmodified clay. This is because the adsorption of anionic polymer in the galleries of bentonite clay keep the interlayer open and allow more water adsorption and swelling property. The authors also investigated the swelling ability, self-healing capacity, and permeability of polymer-modified clay in natural seawater by different techniques such as swell index tests, 1D swell tests in oedometer cells, and hydraulic conductivity tests [211], and the results showed that the swelling property was enhanced with increasing content of polymer present in the bentonite clay. It was reported that another type of bentonite, Ca-bentonite-modified with polymer had values of the hydraulic conductivity 10 times lower than that of pure Ca-bentonite and 5 times lower than that of pure Na-bentonite [212,213].

Innumerable studies were undertaken to test the influence of wet and dry cycles combined with cation exchange on the hydraulic conductivity and the swelling performance of bentonite barriers, and modified bentonite with improved resistance to different environments were developed. It was reported that propylene carbonate (PC) present in the multi-swellable bentonite (MSB) has the capacity to induce the osmotic swelling nature of the clay in pure water and the solution of different electrolytes [214]. Another type of modified clay, dense pre-hydrated GCL (DPH GCL), which is densified by a vacuum extrusion process after pre-hydrating with a polymer solution consisting of Na-CMC, sodium polyacrylate, and methanol, has displayed good resistance to different electrolyte solutions because polymer adsorption onto clay may not be permanent. The performance (self-healing, permeability, hydraulic conductivity, etc.) of GCL structures was improved by changing the structural parameters such as clay type (Na-bentonite, Ca-bentonite), areal density of bentonite, density of GCL, thickness of GCL, texture type (woven or non-woven), and needle punching density [215].

The enhancement of crack resistance of clay by polyester fiber was studied [216]. The influence of polymer fiber content and fiber length on desiccation cracking properties of fiber-reinforced expansive clay was analyzed, and crack parameters (width, space, cell area) were measured and compared with that of pure clay. It was found that polymer fiber-reinforcement into expansive clay reduces the total cracked area, crack intensity factor, average width of crack, space of crack, and the cell area. Studies on the formation and self-healing of desiccation cracks in clays of different plasticities were conducted, and the hydraulic conductivity and self-healing properties were measured [217].

Sato et al. [218] conducted the free swell index test (to avoid time-consuming hydraulic conductivity measurements) in three different liquids (NaCl, leachate, and $CaCl_2$) to study the swelling performance of Na-activated Ca-bentonite subjected to prehydration, followed by modification with different concentrations (0.5, 1.5, and 2%) of two types of polyelectrolyte polymers. It was found that the addition of polymer to bentonite increases the chemical resistance and has less influence on the swelling properties of bentonite, and the modified clay with higher free swell index has lower hydraulic conductivity. A clay that exhibits a free swell index of >20 mL/2 g is good hydraulic barrier with $\kappa < 10^{-9}$ m/s (irrespective of nature of clay and permeating liquid). In order to prevent variations in the hydraulic conductivity of bentonite in various strong inorganic solutions, it was modified with polyacrylic acid [219]. The results showed that

polymer-modified bentonite has greater swellability and maintains lower hydraulic conducting properties than those of pristine Na-bentonite in the presence of inorganic solutions. They also showed good semipermeable membrane properties. Therefore, polymer-modified bentonite can be used as a hydraulic containment barrier.

Mazzoni et al. [220] were investigated influence of different contents of filler on the fatigue, self-healing, and thixotropic properties of aged SBS polymer-modified bitumen. The results revealed that the increasing amount of filler causes unfavorable effects on the mastic fatigue performance, which can be balanced by incorporation of some amount of SBS polymer-modified bitumen, and materials with such properties are expected to be useful for developing sound road pavements. The healing activity of bituminous materials consists of a three-step mechanism: (i) surface route (flow of bitumen under stress), (ii) wetting nature (adhesion of surface of two defect/crack pieces together by surface energy), and (iii) the complete retrieval of mechanical strength. The same group researched the effects of reclaimed asphalt (RA) filler on the fatigue resistance (damage accumulation, viscoelastic behavior, hardness, thixotropy, and healability) of bituminous materials [221]. The high-temperature properties of bituminous materials were improved with the use of different of organophilic MMT as a nano-reinforced filler to pure bitumen, and polyisoprene-modified bitumen, and the effect of MMT on the rheological properties was investigated using oscillatory and creep-recovery tests [222]. The influence of nanosized MMT on the self-healing, compressive strength, and mechanical properties of natural clay soil were investigated, and the results revealed that 5% of nanoclay is the optimized content to improve the self-healing of clay soil [223].

Hosney and Rowe [224] conducted experiments for four years on the trisoplast polymer-improved bentonite–sand mixture (PIBSM) which is used as a cover for gold mines. The results revealed that when PIBSM was in direct with gold mine tailings with millipore water consisting of ionic strength of 145 mmol/L, the mole fraction of bound Na^+ was reduced from 59% to 2%, and κ was improved from 4×10^{-11} to 6.9×10^{-9} m/s. The PIBSM layer served as an excellent barrier to the passage of arsenic (As) heavy-metal ions from the tailings toward the cover soil.

It was reported that GCLs (bentonite-based liners) have the ability to self-heal small cracks or damages that occur during the usage or installation, and the size, distribution, and connectivity of the cracks are controlled by the flow of water and solutes via the clay liners [225,226]. When the water molecules are adsorbed in the damaged area, water plays an important role in the reorganization of networks by bond reformation. Therefore, small defects or damages will be closed under moisture or an aqueous environment.

Mazzieri et al. [227] improved the swelling and chemical compatibility of two types of modified bentonites, multi-swellable bentonite and DPH GCL, in the presence of distilled water and seawater as permeating hydrant liquids. The clay is subtle to the chemical interactions with the hydrating solution. They found that the hydraulic conductivity of both modified bentonites was enhanced by two or three orders of magnitude. It was reported that the valance, concentration, and dielectric constant value of the hydrating liquid effect the expansion of the diffuse double layer (DDL) of negatively charged clays, and as a result the hydraulic conductivity and swelling of the clay are related to the thickness of the DDL [228,229]. The decrease in thickness leads to an increase in hydraulic conductivity, resulting in shrinkage, particle attraction, and the cracking of the clay. When GCLs interacted with different concentration of various electrolyte solutions (NaCl, KCl, and $CaCl_2$) to test the hydraulic conductivity, it was found that the permeability increased up to three orders of magnitude in the electrolyte environment compared with that of pure distilled water [230]. When the concentration of $CaCl_2$ was >50 mM, it led to quick exchange of Na^+ from clay, resulting the hydraulic conductivity of > 10^{-8} cm/s [231]. Hydraulic conductivity tests were conducted on the granular-shaped bentonite in the presence of salt solution (1 M NaCl), and the results showed that the permeability enhanced by two orders of magnitude (>10^{-9} m/s) owing to the saline nature of the solution [232,233].

It was reported that sodium polyacrylate, superabsorbent polymer inclusion in the damaged area, it enhances the self-healing capacity and hydraulic performance of clays [234]. Chai et al. [235] investigated the self-healing performance of GCL using sodium polyacrylate in the presence of different test liquids such as deionized water, NaCl solution and $CaCl_2$ solution. They found that the polymer treated clays exhibited a higher self-healing performance than that the untreated polymer, indicating that polymer provides better performance in the cationic liquid system with higher cation valance and concentrations compared to that of untreated polymer. Sodium polyacrylate was used efficient barrier materials in acidic and alkaline system and improved self-healing capacity of clays [236,237]. Polyacrylate encapsulation into bentonite clay did not change the interlayer spacing of clays [238].

Di et al. [239] reported the fabrication of smart soft material with the combination of clay, poly(N-iso-propylacrylamide) and polydopamine nanoparticles through multiple coordination bonds between them. Resultant material showed excellent rapid self-healing ability, ionic conductivity, non-toxicity, high degree of stretchability, dual thermo- and light-responsiveness activity, and these unique characteristics make them promising candidates for applications in various fields such as wearable devices, soft robotics, soft bioelectronics and other medical applications. Cracks in clays act as linkers to reinforce the polymer network through various forms of hydrogen bonding formation. Poly(N-iso-propylacrylamide) was polymerized into graphene oxide-hectorite clay layers through stepwise in-situ polymerization of monomers and improved their practicality and stability [240]. Polymers encapsulated into cracks of low cost and wide availability of layered silicate based clays and the resultant material showed extraordinary improvement of mechanical, thermal, physical properties (e.g. elasticity, stiff self-healing nature) and healing efficiency due to silicates have anisotropic structure, large surface area, swelling and sorption capacity [241].

LAPONITE is a largely available smecite group of silicate clay and it has physical characteristics such as density of 2.53 g/cm^{-3}, an aspect ratio of 30, and surface area of 350 m^2g^{-1} [242]. Polystyrene microspheres have been used for the modification of LAPONITE through non-covalent bonds to fabricate elastic type materials [243]. Aida et al. [244] developed new class of self-healing material with excellent mechanical strength, which fabricated via new route that consists of four components such as sodium polyacrylate, guanidinium ions (Gu^+) modified-PEG/PEO/ABA triblockcopolyester, water and LAPONITE. Gu ions present in the triblock polymer strongly attach with clay to form crosslinking network via a multivalent salt-bridge involving hydrogen bonding interactions, and produce healable materials. Crack healing efficiency has been improved with polyurethane-based microcapsules modified with isophorone diisocyanate and less content of clay platelets [245]. Yang et al. [246] were developed robust and smart materials with having multifunctional properties such as color tunable luminescence, mechanical strength and high self-healing efficiency at room temperature, using ternary complex of Ln(dpa)3-tpy-mim2 (Ln = Eu, Tb, or Eu or Tb), sodium polyacrylate, PVA and clay in aqueous system. These smart materials showed three different colors such as green, yellow and red under UV light illumination at wavelength of 254 nm.

Nanosized particles as reinforcing fillers in clay materials have received great interest in recent years owing to their unique physico-chemical characteristics, large surface area, stability to chemicals and the environment, and strong ability to greatly improve the properties of clay materials [247,248]. Cracking can be repaired by the reinforcement of carbon nanotubes [249]. Carbon nanofillers were also used to improve the fatigue resistance properties of bituminous materials by means of crack bridging and pull-outs mechanisms [250]. Likewise, various nanoparticles such as carbon fillers, nanoclays, and magnesium alloy were used to study the healing, fatigue, and other properties of different clays through different strategies [29,249,251–256].

5. Assessment of healing efficiency of crack-healed system

Yoon et al. [89] quantitatively determined the healing-efficiency (η) of a material through tensile measurements, as per the equation below.

$$\eta(\%) = (K_{\text{healed}}/K_{\text{pristine}}) \times 100$$

where K is the toughness of the pristine and healed sample.

The tensile tests were performed for prepared photo-healable poly(benzoxazine-propylene oxide) films to estimate the recovery capacity of properties of the films. The healing-efficiency and Young's modulus of the healed specimen were measured to be 96% and 182.3 kPa, respectively [257].

Another research group used optical surface profilometry analysis to investigate the healing-efficiency of a polymer [123]. In this method, the polymer sample was casted on the surface of a glass slide by the drop-casting technique, followed by making a scratch on the polymer film with fine needle of 6 μm depth, as measured by a profilometer. After the completion of healing of the polymer film, the depth of the scratch decreased from 6 μm to 0 μm, demonstrating that the synthesized tri-block copolymers had healing-efficiency of 99.93%.

Another technique was used to evaluate the self-healing properties of the polymer by measuring the permeability test, followed by SEM analysis [152]. The self-healing efficiency of the self-healed material was determined by measuring the interfacial shear strength (IFSS) values [165]. In another method, the healing-efficiency was determined from the ratios of the Young's modulus and fracture stress of the healed material to those of the pristine samples [10]. The closure and sealing of fatigue-induced cracks or damages of structured materials was investigated using a digital microscope with a wide zoom range, followed by rheological studies [170].

Zheng et al. [169] synthesized polymer samples cut into two pieces and brought the cut surfaces of the two pieces together in a tube to heal. They tested the healing-efficiency of the sample by measuring the ratio of the breaking strain of the healed sample to that of the pure polymer sample. The self-healing efficiency of bitumen-based materials was tested using fatigue, fracture, or non-destructive tests. Three- or four-point bending methods or indirect tensile test and dynamic shear rheometry were used to perform the fatigue tests [258–260].

6. Conclusions

The cracks or damages (internal and external) present in clays restrict their applications. Based on previous research studies carried out on this topic, this review showed that results are promising, and such cracks or defects in clays can be healed using various polymers through different polymerization reactions, resulting in crack-healed clays that are fabulous materials with excellent physical, thermal, mechanical, and rheological properties, which make them more advantages for numerous applications in industries.

Clays have crack-healing ability using various polymers by closing cracks or defects, and later rearrangement of polymer networks, indicating the importance of designing and developing novel self-healing polymers. It is also important to test the environmental influence, large-scale production, and cost analysis of clays before and after crack-healing using polymeric and nanomaterials. The influence of different contents of various types of organic polymers and nanoparticles fillers need to be thoroughly analyzed to achieve a detailed understanding of their effects on self-healing properties of crack-healed clays.

Declaration of competing interest

The authors declare that they have no known competing financial interests or personal relationships that could have appeared to influence the work reported in this paper.

Acknowledgment

The authors are grateful to the Australian Research Council (ARC) for the Discovery Grant (DP170104192).

References

[1] M. Morits, et al., Toughness and fracture properties in nacre-mimetic clay/polymer nanocomposites, Adv. Funct. Mater. 27 (10) (2017) 1605378.
[2] K. Saha, K. Dutta, et al., Controlled delivery of tetracycline hydrochloride intercalated into smectite clay using polyurethane nanofibrous membrane for wound healing application, Nano-Struct. Nano-Objects 21 (2020) 100418.
[3] I.R. Kamalieva, I.R. Ishmukhametov, et al., Uptake of halloysite clay nanotubes by human cells: Colourimetric viability tests and microscopy study, Nano-Struct. Nano-Objects 15 (2018) 54–60.
[4] L.A. Shah, et al., Influence of preparation methods on textural properties of purified bentonite, Appl. Clay Sci. 162 (2018) 155–164.
[5] X. Huang, et al., Assembly of large area crack free clay porous films, RSC Adv. 8 (2) (2018) 1001–1004.
[6] U.U. Jadhav, et al., Viability of bacterial spores and crack healing in bacteria-containing geopolymer, Constr. Build. Mater. 169 (2018) 716–723.
[7] S. Sircar, et al., Crack patterns in drying Laponite®-NaCl suspension: Role of the substrate and a static electric field, Langmuir (2018).
[8] Y. Sun, et al., Conformation-directed formation of self-healing diblock copolypeptide hydrogels via polyion complexation, J. Am. Chem. Soc. 139 (42) (2017) 15114–15121.
[9] H. Jiang, et al., Room-temperature self-healing tough nanocomposite hydrogel crosslinked by zirconium hydroxide nanoparticles, Compos. Sci. Technol. 140 (2017) 54–62.
[10] E. Su, O. Okay, Hybrid cross-linked poly (2-acrylamido-2-methyl-1-propanesulfonic acid) hydrogels with tunable viscoelastic, mechanical and self-healing properties, React. Funct. Polym. 123 (2018) 70–79.
[11] R. Guo, et al., Facile access to multisensitive and self-healing hydrogels with reversible and dynamic boronic ester and disulfide linkages, Biomacromolecules 18 (4) (2017) 1356–1364.
[12] Z.P. Zhang, M.Z. Rong, M.Q. Zhang, Mechanically robust, self-healable, and highly stretchable living crosslinked polyurethane based on a reversible C C bond, Adv. Funct. Mater. 28 (11) (2018) 1706050.
[13] Z. Deng, et al., Multifunctional stimuli-responsive hydrogels with self-healing, high conductivity, and rapid recovery through host–guest interactions, Chem. Mater. 30 (5) (2018) 1729–1742.
[14] M. Arslan, et al., Combining benzoxazine and ketene chemistries for self-healing of high performance thermoset surfaces, Polym. Chem. 9 (15) (2018) 2031–2039.
[15] C. Shao, et al., A self-healing cellulose nanocrystal-poly (ethylene glycol) nanocomposite hydrogel via Diels–Alder click reaction, ACS Sustain. Chem. Eng. 5 (7) (2017) 6167–6174.
[16] Y. Liu, et al., Acid–base properties of kaolinite, montmorillonite and illite at marine ionic strength, Chem. Geol. 483 (2018) 191–200.
[17] G.M. Ndzana, et al., Characteristics of clay minerals in soil particles from an argillic horizon of Alfisol in central China, Appl. Clay Sci. 151 (2018) 148–156.

[18] G.B.B. Varadwaj, et al., Facile synthesis of three-dimensional Mg–Al layered double hydroxide/partially reduced graphene oxide nanocomposites for the effective removal of Pb^{2+} from aqueous solution, ACS Appl. Mater. Interfaces 9 (20) (2017) 17290–17305.
[19] S. Ng, J. Plank, Interaction mechanisms between Na montmorillonite clay and MPEG-based polycarboxylate superplasticizers, Cem. Concr. Res. 42 (6) (2012) 847–854.
[20] G. Chen, et al., Anodic stripping voltammetric measurement of trace cadmium at antimony film modified sodium montmorillonite doped carbon paste electrode, Sensors Actuators B 237 (2016) 570–574.
[21] J. Carmona, et al., Rheological and microstructural properties of sepiolite gels. Influence of the addition of ionic surfactants, J. Ind. Eng. Chem. 59 (2018) 1–7.
[22] P. Cheng, et al., Synergetic effects of anhydrite and brucite-periclase materials on phosphate removal from aqueous solution, J. Molecular Liquids 254 (2018) 145–153.
[23] L. Gómez-Hortigüela, M.Á. Camblor, Introduction to the Zeolite Structure-Directing Phenomenon by Organic Species: General Aspects, in: Insights Into the Chemistry of Organic Structure-Directing Agents in the Synthesis of Zeolitic Materials, 2018, pp. 1–41.
[24] R.S. Hebbar, A.M. Isloor, A. Ismail, Preparation and evaluation of heavy metal rejection properties of polyetherimide/porous activated bentonite clay nanocomposite membrane, RSC Adv. 4 (88) (2014) 47240–47248.
[25] A. Abbas, et al., Organoclay-based nanoparticles from montmorillonite and natural clay deposits: Synthesis, characteristics, and application for MTBE removal, Appl. Clay Sci. 142 (2017) 21–29.
[26] J. Scalia IV, C.H. Benson, Hydraulic conductivity of geosynthetic clay liners exhumed from landfill final covers with composite barriers, J. Geotech. Geoenvironmental Eng. 137 (1) (2010) 1–13.
[27] K. Sari, J. Chai, Self healing capacity of geosynthetic clay liners and influencing factors, Geotext. Geomemb. 41 (2013) 64–71.
[28] C.D. Shackelford, G.W. Sevick, G.R. Eykholt, Hydraulic conductivity of geosynthetic clay liners to tailings impoundment solutions, Geotext. Geomemb. 28 (2) (2010) 149–162.
[29] J. He, et al., Effects of leachate infiltration and desiccation cracks on hydraulic conductivity of compacted clay, Water Sci. Eng. 8 (2) (2015) 151–157.
[30] J. Mo, et al., Structure and properties of carbon intercalated halloysite and its organosilicone hybrid film with low dielectric constant, Mater. Des. 128 (2017) 56–63.
[31] O. Poncelet, J. Skrzypski, Industrial Implications in the Uses of Tubular Clay Minerals, in: Developments in Clay Science, Elsevier, 2016, pp. 726–734.
[32] A. Takahara, Y. Higaki, Design and Physicochemical Characterization of Novel Organic–Inorganic Hybrids from Natural Aluminosilicate Nanotubes, in: Functional Polymer Composites with Nanoclays, 2016, pp. 131–156.
[33] B. Ren, J. Sun, S. Bai, Phase transformation and morphology control of zeolite LZ-277 with alkaline media in Na_2O–Al_2O_3–SiO_2–H_2O system, Microporous Mesoporous Mater. 201 (2015) 228–233.
[34] K.A. Sashkina, et al., The effect of H_2O/SiO_2 ratio in precursor solution on the crystal size and morphology of zeolite ZSM-5, Microporous Mesoporous Mater. 244 (2017) 93–100.
[35] C.B. Andrade, S. Toffoli, F.V. Diaz, Adsorption and surface area of modified bentonite used as bleaching clay, in: TMS Annual Meeting & Exhibition, Springer, 2018.
[36] Z. Shu, et al., Preparation of halloysite-derived mesoporous silica nanotube with enlarged specific surface area for enhanced dye adsorption, Appl. Clay Sci. 132 (2016) 114–121.
[37] M. Mahani, et al., Determination of the surface area of mesoporous silicates by X-ray diffraction patterns using partial least squares and multiple linear regressions, Particul. Sci. Technol. 34 (3) (2016) 347–351.
[38] A. Mishra, et al., Effect of different plasmonic metals on photocatalytic degradation of volatile organic compounds (VOCs) by bentonite/M-TiO_2 nanocomposites under UV/visible light, Appl. Clay Sci. 153 (2018) 144–153.
[39] L.A. Galeano, et al., Development of Mn or Fe sulfides in the interlayer space of raw and Al-pillared bentonite, Appl. Clay Sci. 157 (2018) 31–40.
[40] H. Luo, et al., Hydrothermal synthesis of needle-like nanocrystalline zeolites from metakaolin and their applications for efficient removal of organic pollutants and heavy metals, Microporous Mesoporous Mater. 272 (2018) 8–15.
[41] R. Huang, et al., Removal of Cd(II) and Pb(II) from aqueous solution by modified attapulgite clay, Arab. J. Chem. 13 (4) (2020) 4994–5008.
[42] S. Kakaei, et al., Heavy metal removing by modified bentonite and study of catalytic activity, J. Mol. Struct. 1199 (2020).
[43] Z. Su, et al., Coumarin-anchored halloysite nanotubes for highly selective detection and removal of Zn(II), Chem. Eng. J. 393 (2020).
[44] V. Wernert, et al., Cancrinite synthesis from natural kaolinite by high pressure hydrothermal method: Application to the removal of Cd^{2+} and Pb^{2+} from water, Microporous Mesoporous Mater. 301 (2020).
[45] C. Zhang, et al., Characterization and adsorption performance of graphene oxide – montmorillonite nanocomposite for the simultaneous removal of Pb^{2+} and p-nitrophenol, J. Hard Mater. 378 (2019).
[46] W. Dong, et al., A sustainable approach to fabricate new 1D and 2D nanomaterials from natural abundant palygorskite clay for antibacterial and adsorption, Chem. Eng. J. 382 (2020).
[47] A.R. Hamilton, et al., Formulation and antibacterial properties of clay mineral-tetracycline and -doxycycline composites, Appl. Clay Sci. 179 (2019).
[48] L. Zarate-Reyes, et al., Antibacterial clay against gram-negative antibiotic resistant bacteria, J. Hard Mater. 342 (2018) 625–632.
[49] L. Pardo, et al., Adsorption of salmonella in clay minerals and clay-based materials, Minerals 10 (2) (2020) 130.
[50] R. Gao, et al., Layer-by-layer assembly of long-afterglow self-supporting thin films with dual-stimuli-responsive phosphorescence and antiforgery applications, Nano Res. 10 (10) (2017) 3606–3617.
[51] H. Chen, et al., Attapulgite with poly (methylene blue) composite film–Electrocatalytic determination of ascorbic acid, Solid State Sci. 14 (3) (2012) 362–366.
[52] S. Zhang, et al., Novel attapulgite/polyaniline/phosphomolybdic acid–based modified electrode for the electrochemical determination of iodate, J. Electroanal. Soc. 724 (2014) 29–35.
[53] L.B. De Paiva, A.R. Morales, F.R.V. Díaz, Organoclays: properties, preparation and applications, Appl. Clay Sci. 42 (1–2) (2008) 8–24.
[54] Y.-H. Shen, Preparations of organobentonite using nonionic surfactants, Chemosphere 44 (5) (2001) 989–995.
[55] D.J. Chaiko, New poly (ethylene oxide)- Clay composites, Chem. Mater. 15 (5) (2003) 1105–1110.
[56] S. Letaief, C. Detellier, Application of thermal analysis for the characterisation of intercalated and grafted organo-kaolinite nanohybrid materials, J. Therm. Anal. Calorim. 104 (3) (2011) 831–839.
[57] G.K. Dedzo, C. Detellier, Ionic liquid–kaolinite nanohybrid materials for the amperometric detection of trace levels of iodide, Analyst 138 (3) (2013) 767–770.
[58] W. Shen, et al., Grafting of montmorillonite with different functional silanes via two different reaction systems, J. Colloid Interface Sci. 313 (1) (2007) 268–273.
[59] I.K. Tonle, et al., Nanohybrid materials from the grafting of imidazolium cations on the interlayer surfaces of kaolinite. Application as electrode modifier, J. Mater. Chem. 19 (33) (2009) 5996–6003.
[60] I.K. Tonle, et al., Functionalization of natural smectite-type clays by grafting with organosilanes: physico-chemical characterization and application to mercury (II) uptake, Phys. Chem. Chem. Phys. 5 (21) (2003) 4951–4961.
[61] J.C.K. Mbouguen, et al., Electrochemical response of ascorbic and uric acids at organoclay film modified glassy carbon electrodes and sensing applications, Talanta 85 (1) (2011) 754–762.
[62] D.E. Bayraktepe, Z. Yazan, K. Polat, Sensitive and selective voltammetric determination of anti- cancer agent shikonin on sepiolite clay/TiO_2 nanoparticle/MWCNTs composite carbon paste sensor and investigation of its electro- oxidation mechanism, J. Electroanal. Soc. 780 (2016) 38–45.
[63] P. Banković, et al., Mixed pillared bentonite for electrooxidation of phenol, Appl. Clay Sci. 49 (1–2) (2010) 84–89.
[64] U.P. Azad, et al., Tris (1, 10-phenanthroline) iron (II)-bentonite film as efficient electrochemical sensing platform for nitrite determination, Electrochim. Acta 127 (2014) 193–199.
[65] D. Tiwari, S.M. Lee, Fabrication of efficient and selective total arsenic sensor using the hybrid materials modified carbon paste electrodes, J. Electroanal. Soc. 784 (2017) 109–114.
[66] A. Sharma, et al., Studies on clay-gelatin nanocomposite as urea sensor, Appl. Clay Sci. 146 (2017) 297–305.
[67] Y. Wen, et al., Simultaneous analysis of uric acid, xanthine and hypoxanthine using voltammetric sensor based on nanocomposite of palygorskite and nitrogen doped graphene, J. Electroanal. Soc. 805 (2017) 159–170.
[68] M.C. dos Santos, et al., External stimulus-responsive interfaces in polymer nanocomposites, Polym. Compos. 37 (5) (2016) 1342–1349.
[69] N. Roy, E. Buhler, J.M. Lehn, The tris-urea motif and its incorporation into polydimethylsiloxane-based supramolecular materials presenting self-healing features, Chem. Eur. J. 19 (27) (2013) 8814–8820.
[70] S. White, et al., Restoration of large damage volumes in polymers, Science 344 (6184) (2014) 620–623.
[71] Y.-L. Rao, et al., Stretchable self-healing polymeric dielectrics cross-linked through metal–ligand coordination, J. Am. Chem. Soc. 138 (18) (2016) 6020–6027.
[72] H. Chen, et al., A rapidly self-healing supramolecular polymer hydrogel with photostimulated room-temperature phosphorescence responsiveness, Angew. Chem. Int. Ed. 53 (51) (2014) 14149–14152.
[73] M.Q. Zhang, M.Z. Rong, Theoretical consideration and modeling of self-healing polymers, J. Polym. Sci. B 50 (4) (2012) 229–241.
[74] C. Cheng, et al., Renewable eugenol-based functional polymers with self-healing and high temperature resistance properties, J. Polym. Res. 25 (2) (2018) 57.

[75] W.M. Xu, M.Z. Rong, M.Q. Zhang, Sunlight driven self-healing, reshaping and recycling of a robust, transparent and yellowing-resistant polymer, J. Mater. Chem. A 4 (27) (2016) 10683–10690.
[76] M. Arslan, B. Kiskan, Y. Yagci, Recycling and self-healing of polybenzoxazines with dynamic sulfide linkages, Sci. Rep. 7 (1) (2017) 5207.
[77] Y.-L. Liu, T.-W. Chuo, Self-healing polymers based on thermally reversible Diels–Alder chemistry, Polym. Chem. 4 (7) (2013) 2194–2205.
[78] J. Ling, M.Z. Rong, M.Q. Zhang, Coumarin imparts repeated photochemical remendability to polyurethane, J. Mater. Chem. 21 (45) (2011) 18373–18380.
[79] J. Ling, M.Z. Rong, M.Q. Zhang, Photo-stimulated self-healing polyurethane containing dihydroxyl coumarin derivatives, Polymer 53 (13) (2012) 2691–2698.
[80] Y.H. Zhao, et al., Photoinitiated thiol–epoxy addition for the preparation of photoinduced self-healing fatty coatings, RSC Adv. 6 (38) (2016) 32098–32105.
[81] B. Kiskan, Y. Yagci, Self-healing of poly (propylene oxide)-polybenzoxazine thermosets by photoinduced coumarine dimerization, J. Polym. Sci. A 52 (20) (2014) 2911–2918.
[82] Q. Yan, et al., Redox-switchable supramolecular polymers for responsive self-healing nanofibers in water, Polym. Chem. 4 (4) (2013) 1216–1220.
[83] L.-P. Lv, et al., Redox responsive release of hydrophobic self-healing agents from polyaniline capsules, J. Am. Chem. Soc. 135 (38) (2013) 14198–14205.
[84] K.S. Toohey, et al., Delivery of two-part self-healing chemistry via microvascular networks, Adv. Funct. Mater. 19 (9) (2009) 1399–1405.
[85] M.D. Hager, et al., Self-healing materials, Adv. Mater. 22 (47) (2010) 5424–5430.
[86] B. Sandmann, et al., Metallopolymers as an emerging class of self-healing materials, in: Hierarchical Macromolecular Structures: 60 Years After the Staudinger Nobel Prize II, Springer, 2013, pp. 239–257.
[87] P. Cordier, et al., Self-healing and thermoreversible rubber from supramolecular assembly, Nature 451 (7181) (2008) 977.
[88] A. Susa, et al., Effect of the dianhydride/branched diamine ratio on the architecture and room temperature healing behavior of polyetherimides, ACS Appl. Mater. Interfaces 8 (49) (2016) 34068–34079.
[89] J.A. Yoon, et al., Self-healing polymer films based on thiol–disulfide exchange reactions and self-healing kinetics measured using atomic force microscopy, Macromolecules 45 (1) (2011) 142–149.
[90] M. AbdolahZadeh, et al., Healable dual organic–inorganic crosslinked sol–gel based polymers: crosslinking density and tetrasulfide content effect, J. Polym. Sci. A 52 (14) (2014) 1953–1961.
[91] O.R. Cromwell, J. Chung, Z. Guan, Malleable and self-healing covalent polymer networks through tunable dynamic boronic ester bonds, J. Am. Chem. Soc. 137 (20) (2015) 6492–6495.
[92] S.J. Garcia, Effect of polymer architecture on the intrinsic self-healing character of polymers, Eur. Polym. J. 53 (2014) 118–125.
[93] A. Rekondo, et al., Catalyst-free room-temperature self-healing elastomers based on aromatic disulfide metathesis, Mater. Horiz. 1 (2) (2014) 237–240.
[94] R. Martin, et al., The processability of a poly (urea-urethane) elastomer reversibly crosslinked with aromatic disulfide bridges, J. Mater. Chem. A 2 (16) (2014) 5710–5715.
[95] A. Grande, et al., Effect of the polymer structure on the viscoelastic and interfacial healing behaviour of poly (urea-urethane) networks containing aromatic disulphides, Eur. Polym. J. 97 (2017) 120–128.
[96] Y. Wang, et al., Transparent, healable elastomers with high mechanical strength and elasticity derived from hydrogen-bonded polymer complexes, ACS Appl. Mater. Interfaces 9 (34) (2017) 29120–29129.
[97] Y. Yang, X. Lu, W. Wang, A tough polyurethane elastomer with self-healing ability, Mater. Des. 127 (2017) 30–36.
[98] Y. Xiao, H. Huang, X. Peng, Synthesis of self-healing waterborne polyurethanes containing sulphonate groups, RSC Adv. 7 (33) (2017) 20093–20100.
[99] A. Grande, et al., A combined fracture mechanical–rheological study to separate the contributions of hydrogen bonds and disulphide linkages to the healing of poly (urea-urethane) networks, Polymer 96 (2016) 26–34.
[100] Y. Takashima, et al., Supramolecular materials cross-linked by host–guest inclusion complexes: the effect of side chain molecules on mechanical properties, Macromolecules 50 (8) (2017) 3254–3261.
[101] R. Martin, et al., Dynamic sulfur chemistry as a key tool in the design of self-healing polymers, Smart Mater. Struct. 25 (8) (2016) 084017.
[102] D. Ramachandran, F. Liu, M.W. Urban, Self-repairable copolymers that change color, RSC Adv. 2 (1) (2012) 135–143.
[103] Y.J. Kim, P.H. Huh, B.K. Kim, Synthesis of self-healing polyurethane urea-based supramolecular materials, J. Polym. Sci. B 53 (7) (2015) 468–474.
[104] L. Wang, et al., An injectable, dual responsive, and self-healing hydrogel based on oxidized sodium alginate and hydrazide-modified poly (ethyleneglycol), Molecules 23 (3) (2018) 546.
[105] D. Döhler, H. Peterlik, W.H. Binder, A dual crosslinked self-healing system: supramolecular and covalent network formation of four-arm star polymers, Polymer 69 (2015) 264–273.
[106] C. Cheng, et al., Self-healing polymers based on a photo-active reversible addition-fragmentation chain transfer (RAFT) agent, J. Polym. Res. 22 (4) (2015) 46.
[107] F. Potier, et al., Nano-building block based-hybrid organic–inorganic copolymers with self-healing properties, Polym. Chem. 5 (15) (2014) 4474–4479.
[108] H. Ying, Y. Zhang, J. Cheng, Dynamic urea bond for the design of reversible and self-healing polymers, Nature Commun. 5 (2014) 3218.
[109] Z. Zhao, et al., Preparation of periodic copolymers by living anionic polymerization mechanism assisted with a versatile programmed monomer addition mode, Polymer 137 (2018) 364–369.
[110] J. Huang, et al., Precisely controlled polymerization of styrene and conjugated dienes by group 3 single-site catalysts, ChemCatChem 10 (1) (2018) 42–61.
[111] S. Li, et al., Development of Group 3 Catalysts for Alternating Copolymerization of Ethylene and Styrene Derivatives, ACS Catal. (2018).
[112] W. Fan, et al., Living ab initio emulsion polymerization of methyl methacrylate in water using a water-soluble organotellurium chain transfer agent under thermal and photochemical conditions, Angew. Chem. Int. Ed. 57 (4) (2018) 962–966.
[113] J. Chen, et al., Facile preparation of fluorescent nanodiamond-based polymer composites through a metal-free photo-initiated RAFT process and their cellular imaging, Chem. Eng. J. 337 (2018) 82–90.
[114] Q. Wan, et al., Aggregation-induced emission active luminescent polymeric nanoparticles: non-covalent fabrication methodologies and biomedical applications, Appl. Mater. Today 9 (2017) 145–160.
[115] R. Jiang, et al., A facile one-pot Mannich reaction for the construction of fluorescent polymeric nanoparticles with aggregation-induced emission feature and their biological imaging, Mater. Sci. Eng. C 81 (2017) 416–421.
[116] X. Zhang, et al., Polymeric AIE-based nanoprobes for biomedical applications: recent advances and perspectives, Nanoscale 7 (27) (2015) 11486–11508.
[117] Y. Liu, et al., A facile strategy for fabrication of aggregation-induced emission (AIE) active fluorescent polymeric nanoparticles (FPNs) via post modification of synthetic polymers and their cell imaging, Mater. Sci. Eng. C 79 (2017) 590–595.
[118] N. Usuki, K. Satoh, M. Kamigaito, Synthesis of isotactic-block-syndiotactic poly (methyl methacrylate) via stereospecific living anionic polymerizations in combination with metal-halogen exchange, halogenation, and click reactions, Polymers 9 (12) (2017) 723.
[119] Y.-G. Yu, et al., Precise synthesis of bottlebrush block copolymers from ω-end-norbornyl polystyrene and poly (4-tert-butoxystyrene) via living anionic polymerization and ring-opening metathesis polymerization, Macromolecules (2018).
[120] F. Zhong, et al., Allylthioketone mediated free radical polymerization of methacrylates, Polymers 9 (11) (2017) 608.
[121] A. Tochwin, et al., Thermoresponsive and reducible hyperbranched polymers synthesized by RAFT polymerisation, Polymers 9 (9) (2017) 443.
[122] S.L. Banerjee, et al., A self-healable fluorescence active hydrogel based on ionic block copolymers prepared via ring opening polymerization and xanthate mediated RAFT polymerization, Polym. Chem. 9 (10) (2018) 1190–1205.
[123] N.B. Pramanik, et al., A new class of self-healable hydrophobic materials based on ABA triblock copolymer via RAFT polymerization and Diels–Alder click chemistry, Polymer 119 (2017) 195–205.
[124] D. Döhler, P. Zare, W. Binder, Hyperbranched polyisobutylenes for self-healing polymers, Polym. Chem. 5 (3) (2014) 992–1000.
[125] T.C. Mauldin, et al., Modified rheokinetic technique to enhance the understanding of microcapsule-based self-healing polymers, ACS Appl. Mater. Interfaces 4 (3) (2012) 1831–1837.
[126] D.A. McIlroy, et al., Microencapsulation of a reactive liquid-phase amine for self-healing epoxy composites, Macromolecules 43 (4) (2010) 1855–1859.
[127] M. Keller, S. White, N. Sottos, Torsion fatigue response of self-healing poly (dimethylsiloxane) elastomers, Polymer 49 (13–14) (2008) 3136–3145.
[128] S. Billiet, et al., Development of optimized autonomous self-healing systems for epoxy materials based on maleimide chemistry, Polymer 53 (12) (2012) 2320–2326.
[129] Q.-y. Cao, et al., Preparation of AIE-active fluorescent polymeric nanoparticles through a catalyst-free thiol-yne click reaction for bioimaging applications, Mater. Sci. Eng. C 80 (2017) 411–416.
[130] L. Huang, et al., A facile surface modification strategy for fabrication of fluorescent silica nanoparticles with the aggregation-induced emission dye through surface-initiated cationic ring opening polymerization, Mater. Sci. Eng. C 94 (2019) 270–278.

[131] R. Jiang, et al., Facile fabrication of organic dyed polymer nanoparticles with aggregation-induced emission using an ultrasound-assisted multi-component reaction and their biological imaging, J. Colloid Interface Sci. 519 (2018) 137–144.
[132] J. Tian, et al., Synthesis and cell imaging applications of amphiphilic AIE-active poly (amino acid) s, Mater. Sci. Eng. C 79 (2017) 563–569.
[133] Z. Long, et al., Facile synthesis of AIE-active amphiphilic polymers: self-assembly and biological imaging applications, Mater. Sci. Eng. C 66 (2016) 215–220.
[134] H. Huang, et al., Facile modification of nanodiamonds with hyperbranched polymers based on supramolecular chemistry and their potential for drug delivery, J. Colloid Interface Sci. 513 (2018) 198–204.
[135] H. Huang, et al., Direct encapsulation of AIE-active dye with β cyclodextrin terminated polymers: Self-assembly and biological imaging, Mater. Sci. Eng. C 78 (2017) 862–867.
[136] Z. Long, et al., Marrying multicomponent reactions and aggregation-induced emission (AIE): new directions for fluorescent nanoprobes, Polym. Chem. 8 (37) (2017) 5644–5654.
[137] Z. Long, et al., Preparation of water soluble and biocompatible AIE-active fluorescent organic nanoparticles via multicomponent reaction and their biological imaging capability, Chem. Eng. J. 308 (2017) 527–534.
[138] Q.-y. Cao, et al., Microwave-assisted multicomponent reactions for rapid synthesis of AIE-active fluorescent polymeric nanoparticles by post-polymerization method, Mater. Sci. Eng. C 80 (2017) 578–583.
[139] R. Jiang, et al., Facile fabrication of luminescent polymeric nanoparticles containing dynamic linkages via a one-pot multicomponent reaction: synthesis, aggregation-induced emission and biological imaging, Mater. Sci. Eng. C 80 (2017) 708–714.
[140] X. Zhang, et al., Fabrication of aggregation induced emission dye-based fluorescent organic nanoparticles via emulsion polymerization and their cell imaging applications, Polym. Chem. 5 (2) (2014) 399–404.
[141] F. Herbst, S. Seiffert, W.H. Binder, Dynamic supramolecular poly (isobutylene) s for self-healing materials, Polym. Chem. 3 (11) (2012) 3084–3092.
[142] M.J. Barthel, et al., Self-healing materials via reversible crosslinking of poly (ethylene oxide)-block-poly (furfuryl glycidyl ether)(peo-b-pfge) block copolymer films, Adv. Funct. Mater. 23 (39) (2013) 4921–4932.
[143] B.J. Saikia, S.K. Dolui, Designing semiencapsulation based covalently self-healable poly (methyl methacrylate) composites by Atom Transfer Radical Polymerization, J. Polym. Sci. A 54 (12) (2016) 1842–1851.
[144] H. Liu, H. Chung, Self-healing properties of lignin-containing nanocomposite: Synthesis of lignin-graft-poly (5-acetylaminopentyl acrylate) via raft and click chemistry, Macromolecules 49 (19) (2016) 7246–7256.
[145] C.-H. Li, et al., A highly stretchable autonomous self-healing elastomer, Nature Chem. 8 (6) (2016) 618.
[146] B. Radi, R.M. Wellard, G.A. George, Effect of dangling chains on the structure and physical properties of a tightly crosslinked poly (ethylene glycol) network, Soft Matter 9 (12) (2013) 3262–3271.
[147] Y.M. Boiko, On the molecular mechanism of self-healing of glassy polymers, Colloid Polym. Sci. 294 (7) (2016) 1237–1242.
[148] X. Huang, M.J. Bolen, N.S. Zacharia, Silver nanoparticle aided self-healing of polyelectrolyte multilayers, Phys. Chem. Chem. Phys. 16 (22) (2014) 10267–10273.
[149] M. Lefort, et al., Nanosized films based on multicharged small molecules and oppositely charged polyelectrolytes obtained by simultaneous spray coating of interacting species, Langmuir 29 (47) (2013) 14536–14544.
[150] C. Elosua, et al., Comparative study of layer-by-layer deposition techniques for poly (sodium phosphate) and poly (allylamine hydrochloride), Nanoscale Res. Lett. 8 (1) (2013) 539.
[151] E. Ortega, et al., Spray-assisted layer-by-layer assembly of decorated PEI/PAA films: morphological, growth and mechanical behavior, J. Coat. Technol. Res. 14 (4) (2017) 927–935.
[152] B.A. Getachew, S.-R. Kim, J.-H. Kim, Self-healing hydrogel pore-filled water filtration membranes, Environ. Sci. Technol. 51 (2) (2017) 905–913.
[153] H. Zhang, H. Xia, Y. Zhao, Poly (vinyl alcohol) hydrogel can autonomously self-heal, ACS Macro Lett. 1 (11) (2012) 1233–1236.
[154] J. Cui, A. del Campo, Multivalent H-bonds for self-healing hydrogels, Chem. Commun. 48 (74) (2012) 9302–9304.
[155] D.C. Tuncaboylu, et al., Autonomic self-healing in covalently crosslinked hydrogels containing hydrophobic domains, Polymer 54 (23) (2013) 6381–6388.
[156] B.K. Ahn, et al., Surface-initiated self-healing of polymers in aqueous media, Nature Mater. 13 (9) (2014) 867.
[157] M.Q. Zhang, M.Z. Rong, Intrinsic self-healing of covalent polymers through bond reconnection towards strength restoration, Polym. Chem. 4 (18) (2013) 4878–4884.
[158] C.e. Yuan, et al., Self-healing of polymers via synchronous covalent bond fission/radical recombination, Chem. Mater. 23 (22) (2011) 5076–5081.
[159] S. Jung, et al., A new reactive polymethacrylate bearing pendant furfuryl groups: Synthesis, thermoreversible reactions, and self-healing, Polymer 109 (2017) 58–65.
[160] S. Cao, et al., A thermal self-healing polyurethane thermoset based on phenolic urethane, Polym. J. 49 (11) (2017) 775.
[161] G.A. Barcan, X. Zhang, R.M. Waymouth, Structurally dynamic hydrogels derived from 1, 2-dithiolanes, J. Am. Chem. Soc. 137 (17) (2015) 5650–5653.
[162] S. Telitel, et al., Introduction of self-healing properties into covalent polymer networks via the photodissociation of alkoxyamine junctions, Polym. Chem. 5 (3) (2014) 921–930.
[163] J. Su, et al., Reversible cross-linking of hydrophilic dynamic covalent polymers with radically exchangeable alkoxyamines in aqueous media, Polym. Chem. 2 (9) (2011) 2021–2026.
[164] S. Itoh, et al., Spontaneous crack healing in nanostructured silica-based thin films, ACS Nano 11 (10) (2017) 10289–10294.
[165] Z. Hu, et al., Light triggered interfacial damage self-healing of poly (p-phenylene benzobisoxazole) fiber composites, Nanotechnology 29 (18) (2018) 185602.
[166] W. Qin, et al., Modifying the carbon fiber–epoxy matrix interphase with silicon dioxide nanoparticles, RSC Adv. 5 (4) (2015) 2457–2465.
[167] Z. Hu, et al., Light-triggered C 60 release from a graphene/cyclodextrin nanoplatform for the protection of cytotoxicity induced by nitric oxide, J. Mater. Chem. B (2018).
[168] L. Huang, et al., Multichannel and repeatable self-healing of mechanical enhanced graphene-thermoplastic polyurethane composites, Adv. Mater. 25 (15) (2013) 2224–2228.
[169] J. Zheng, et al., Mechanical robust and self-healable supramolecular hydrogel, Macromol. Rapid Commun. 37 (3) (2016) 265–270.
[170] W. Post, et al., Healing of early stage fatigue damage in ionomer/fe3o4 nanoparticle composites, Polymers 8 (12) (2016) 436.
[171] H. Xuan, et al., Self-Healing, antibacterial and sensing nanoparticle coating and its excellent optical applications, Sensors Actuators B (2017).
[172] Y. Li, et al., Highly transparent, nanofiller-reinforced scratch-resistant polymeric composite films capable of healing scratches, ACS Nano 9 (10) (2015) 10055–10065.
[173] A. Fereidoon, M.G. Ahangari, M. Jahanshahi, Effect of nanoparticles on the morphology and thermal properties of self-healing poly (urea-formaldehyde) microcapsules, J. Polym. Res. 20 (6) (2013) 151.
[174] Y. Zhou, M. Zhu, S. Li, Self-switchable catalysis by a nature-inspired polymer nanoreactor containing Pt nanoparticles, J. Mater. Chem. A 2 (19) (2014) 6834–6839.
[175] C.C. Neikirk, J.W. Chung, R.D. Priestley, Thermomechanical behavior of hydrogen-bond based supramolecular poly (ε-caprolactone)-silica nanocomposites, RSC Adv. 3 (37) (2013) 16686–16696.
[176] Y. Chen, Z. Guan, Self-assembly of core–shell nanoparticles for self-healing materials, Polym. Chem. 4 (18) (2013) 4885–4889.
[177] E.A. Appel, et al., Exploiting electrostatic interactions in polymer–nanoparticle hydrogels, ACS Macro Lett. 4 (8) (2015) 848–852.
[178] L. Huang, et al., Recent advances and progress on melanin-like materials and their biomedical applications, Biomacromolecules 19 (6) (2018) 1858–1868.
[179] M. Liu, et al., Recent developments in polydopamine: an emerging soft matter for surface modification and biomedical applications, Nanoscale 8 (38) (2016) 16819–16840.
[180] Y. Shi, et al., Facile synthesis of polymeric fluorescent organic nanoparticles based on the self-polymerization of dopamine for biological imaging, Mater. Sci. Eng. C 77 (2017) 972–977.
[181] D. Gan, et al., Facile preparation of functionalized carbon nanotubes with tannins through mussel-inspired chemistry and their application in removal of methylene blue, J. Molecular Liquids 271 (2018) 246–253.
[182] M. Liu, et al., Self-polymerization of dopamine and polyethyleneimine: novel fluorescent organic nanoprobes for biological imaging applications, J. Mater. Chem. B 3 (17) (2015) 3476–3482.
[183] Y. Shi, et al., Recent progress and development on polymeric nanomaterials for photothermal therapy: a brief overview, J. Mater. Chem. B 5 (2) (2017) 194–206.
[184] X. Zhang, et al., Mussel-inspired fabrication of functional materials and their environmental applications: progress and prospects, Appl. Mater. Today 7 (2017) 222–238.
[185] Y. Liu, K. Ai, L. Lu, Polydopamine and its derivative materials: synthesis and promising applications in energy, environmental, and biomedical fields, Chem. Rev. 114 (9) (2014) 5057–5115.
[186] Q. Huang, et al., Preparation of polyethylene polyamine@tannic acid encapsulated MgAl-layered double hydroxide for the efficient removal of copper (II) ions from aqueous solution, J. Taiwan Inst. Chem. Eng. 82 (2018) 92–101.
[187] H. Huang, et al., Facile fabrication of glycosylated and PEGylated carbon nanotubes through the combination of mussel inspired chemistry and surface-initiated ATRP, Mater. Sci. Eng. C 106 (2020) 110157.
[188] Q. Huang, et al., Surface functionalized SiO_2 nanoparticles with cationic polymers via the combination of mussel inspired chemistry and surface initiated atom transfer radical polymerization: characterization and enhanced removal of organic dye, J. Colloid Interface Sci. 499 (2017) 170–179.

[189] G. Zeng, et al., Rapid synthesis of MoS_2-PDA-Ag nanocomposites as heterogeneous catalysts and antimicrobial agents via microwave irradiation, Appl. Surf. Sci. 459 (2018) 588–595.
[190] D. Gan, et al., Bioinspired functionalization of MXenes (Ti_3C_2TX) with amino acids for efficient removal of heavy metal ions, Appl. Surf. Sci. 504 (2020) 144603.
[191] Q. Huang, et al., Facile preparation of polyethylenimine-tannins coated SiO2 hybrid materials for Cu^{2+} removal, Appl. Surf. Sci. 427 (2018) 535–544.
[192] X. Zhang, et al., Preparation of amine functionalized carbon nanotubes via a bioinspired strategy and their application in Cu^{2+} removal, Appl. Surf. Sci. 343 (2015) 19–27.
[193] L. Guo, et al., Surface modification of carbon nanotubes with polyethyleneimine through mussel inspired chemistry and Mannich reaction for adsorptive removal of copper ions from aqueous solution, J. Environ. Chem. Eng. 8 (3) (2020) 103721.
[194] J. Dou, et al., Functionalization of carbon nanotubes with chitosan based on MALI multicomponent reaction for Cu^{2+} removal, Int. J. Biol. Macromol. 136 (2019) 476–485.
[195] J. Dou, et al., Preparation of polymer functionalized layered double hydroxide through mussel-inspired chemistry and Kabachnik–Fields reaction for highly efficient adsorption, J. Environ. Chem. Eng. 8 (1) (2020) 103634.
[196] Q. Huang, et al., Synthesis of polyacrylamide immobilized molybdenum disulfide (MoS_2@PDA@PAM) composites via mussel-inspired chemistry and surface-initiated atom transfer radical polymerization for removal of copper (II) ions, J. Taiwan Inst. Chem. Eng. 86 (2018) 174–184.
[197] G. Zeng, et al., Surface modification and drug delivery applications of MoS_2 nanosheets with polymers through the combination of mussel inspired chemistry and SET-LRP, J. Taiwan Inst. Chem. Eng. 82 (2018) 205–213.
[198] D. Gan, et al., Carbon nanotubes-based polymer nanocomposites: Biomimic preparation and methylene blue adsorption, J. Environ. Chem. Eng. (2019) 103525.
[199] S.-H. Lee, S.-R. Shin, D.-S. Lee, Self-healing of cross-linked PU via dual-dynamic covalent bonds of a schiff base from cystine and vanillin, Mater. Des. 172 (2019) 107774.
[200] C. Luo, et al., Biocompatible self-healing coating based on schiff base for promoting adhesion of coral cells, ACS Appl. Bio Mater. 3 (3) (2020) 1481–1495.
[201] M. Vahedi, et al., Self-healing, injectable gelatin hydrogels cross-linked by dynamic schiff base linkages support cell adhesion and sustained release of antibacterial drugs, Macromol. Mater. Eng. 303 (9) (2018) 1800200.
[202] J. Ren, H. Xuan, L. Ge, Double network self-healing chitosan/dialdehyde starch-polyvinyl alcohol film for gas separation, Appl. Surf. Sci. 469 (2019) 213–219.
[203] L. Tang, et al., Metallo-supramolecular hydrogels based on amphiphilic polymers bearing a hydrophobic schiff base ligand with rapid self-healing and multi-stimuli responsive properties, Polym. Chem. 8 (32) (2017) 4680–4687.
[204] J. Ren, H. Xuan, L. Ge, Colorful self-healing polyelectrolyte nano-film based on schiff base linkage capable of sensing, Eur. Polym. J. 93 (2017) 521–529.
[205] H. Li, et al., Environmental friendly polymers based on schiff-base reaction with self-healing, remolding and degradable ability, Polymer 85 (2016) 106–113.
[206] S. Krisnanto, et al., Water content of soil matrix during lateral water flow through cracked soil, Eng. Geol. 210 (2016) 168–179.
[207] W. Nakao, et al., Critical crack-healing condition for SiC whisker reinforced alumina under stress, J. Eur. Ceram. Soc. 25 (16) (2005) 3649–3655.
[208] S.D. Nielsen, et al., Constraints on $CaCO_3$ precipitation in superabsorbent polymer by aerobic bacteria, Appl. Microbiol. Biotechnol. 104 (1) (2020) 365–375.
[209] S. Han, et al., Effectiveness of expanded clay as a bacteria carrier for self-healing concrete, Appl. Biol. Chem. 62 (1) (2019) 19.
[210] M. De Camillis, et al., Effect of wet-dry cycles on polymer treated bentonite in seawater: swelling ability, hydraulic conductivity and crack analysis, Appl. Clay Sci. 142 (2017) 52–59.
[211] M. De Camillis, et al., Hydraulic conductivity and swelling ability of a polymer modified bentonite subjected to wet–dry cycles in seawater, Geotext. Geomemb. 44 (5) (2016) 739–747.
[212] G. Di Emidio, et al., Polymer-treated bentonite clay for chemical-resistant geosynthetic clay liners, Geosynth. Int. 22 (1) (2015) 125–137.
[213] G. Di Emidio, et al., Beneficial impact of polymer treatment of Ca-bentonites on long term hydraulic conductivity, in: 10th International Conference on Geosynthetics, IGS-2014, DGGT, 2014.
[214] M. Kondo, Method of activation of clay and activated clay, 1996, Google Patents.
[215] F. Parastar, et al., A parametric study on hydraulic conductivity and self-healing properties of geotextile clay liners used in landfills, J. Environ. Manag. 202 (2017) 29–37.
[216] U. Chaduvula, B. Viswanadham, J. Kodikara, A study on desiccation cracking behavior of polyester fiber-reinforced expansive clay, Appl. Clay Sci. 142 (2017) 163–172.
[217] J.C. Cripps, K.K. Parmar, Investigations into the self-healing of desiccation cracks in compacted clays, in: Engineering Geology for Society and Territory-Volume 5, Springer, 2015, pp. 1327–1331.
[218] K. Sato, et al., Comparison of prehydration and polymer adding effects on Na activated Ca-bentonite by free swell index test, Appl. Clay Sci. 142 (2017) 69–80.
[219] J. Scalia IV, et al., Long-term hydraulic conductivity of a bentonite-polymer composite permeated with aggressive inorganic solutions, J. Geotech. Geoenvironmental Eng. 140 (3) (2013) 04013025.
[220] G. Mazzoni, et al., Fatigue, self-healing and thixotropy of bituminous mastics including aged modified bitumens and different filler contents, Constr. Build. Mater. 131 (2017) 496–502.
[221] G. Mazzoni, A. Stimilli, F. Canestrari, Self-healing capability and thixotropy of bituminous mastics, Int. J. Fatigue 92 (2016) 8–17.
[222] E. Santagata, et al., Bituminous-based nanocomposites with improved high-temperature properties, Composites B 99 (2016) 9–16.
[223] M. Mohammadi, A.J. Choobbasti, The effect of self-healing process on the strength increase in clay, J. Adhes. Sci. Technol. 32 (16) (2018) 1750–1772.
[224] M. Hosney, R.K. Rowe, Performance of polymer-enhanced bentonite–sand mixture for covering arsenic-rich gold mine tailings for up to 4 years, Can. Geotech. J. 54 (4) (2016) 588–599.
[225] J.-C. Chai, et al., Predicting self-healing ratio of GCL with a damage hole, Geotext. Geomemb. 44 (5) (2016) 761–769.
[226] C.-S. Tang, et al., Experimental characterization of shrinkage and desiccation cracking in thin clay layer, Appl. Clay Sci. 52 (1–2) (2011) 69–77.
[227] F. Mazzieri, G. Di Emidio, E. Pasqualini, Effect of wet-and-dry ageing in seawater on the swelling properties and hydraulic conductivity of two amended bentonites, Appl. Clay Sci. 142 (2017) 40–51.
[228] C.D. Shackelford, et al., Evaluating the hydraulic conductivity of GCLs permeated with non-standard liquids, Geotext. Geomemb. 18 (2–4) (2000) 133–161.
[229] S.R. Meer, C.H. Benson, Hydraulic conductivity of geosynthetic clay liners exhumed from landfill final covers, J. Geotech. Geoenvironmental Eng. 133 (5) (2007) 550–563.
[230] H.Y. Jo, et al., Long-term hydraulic conductivity of a geosynthetic clay liner permeated with inorganic salt solutions, J. Geotech. Geoenvironmental Eng. 131 (4) (2005) 405–417.
[231] H.Y. Jo, et al., Hydraulic conductivity and swelling of nonprehydrated GCLs permeated with single-species salt solutions, J. Geotech. Geoenvironmental Eng. 127 (7) (2001) 557–567.
[232] T. Katsumi, et al., Long-term barrier performance of modified bentonite materials against sodium and calcium permeant solutions, Geotext. Geomemb. 26 (1) (2008) 14–30.
[233] C.-M. Zhu, et al., Influence of salt solutions on the swelling pressure and hydraulic conductivity of compacted GMZ01 bentonite, Eng. Geol. 166 (2013) 74–80.
[234] N. Salemi, et al., Geosynthetic clay liners: effect of structural properties and additives on hydraulic performance and durability, Environ. Earth Sci. 77 (5) (2018) 168.
[235] J.-C. Chai, N. Prongmanee, Barrier properties of a geosynthetic clay liner using polymerized sodium bentonite, Geotext. Geomemb. (2020).
[236] N. Prongmanee, J.-C. Chai, Performance of geosynthetic clay liner with polymerized bentonite in highly acidic or alkaline solutions, Int. J. Geosynth. Ground Eng. 5 (3) (2019) 26.
[237] N. Salemi, et al., Improving hydraulic performance and durability of sandwich clay liner using super-absorbent polymer, J. Sandw. Struct. Mater. 21 (3) (2019) 1055–1071.
[238] N. Prongmanee, J.-C. Chai, S. Shen, Hydraulic properties of polymerized bentonites, J. Mater. Civ. Eng. 30 (10) (2018) 04018247.
[239] X. Di, et al., Poly (N-isopropylacrylamide)/polydopamine/clay nanocomposite hydrogels with stretchability, conductivity, and dual light-and thermo-responsive bending and adhesive properties, Colloids Surfaces B 177 (2019) 149–159.
[240] E. Zhang, et al., Infrared-driving actuation based on bilayer graphene oxide-poly (N-isopropylacrylamide) nanocomposite hydrogels, J. Mater. Chem. A 2 (37) (2014) 15633–15639.
[241] S. Li, et al., Illustration and application of enhancing effect of arginine on interactions between nano-clays: self-healing hydrogels, Soft Matter 15 (2) (2019) 303–311.
[242] R.K. Pujala, N. Pawar, H. Bohidar, Universal sol state behavior and gelation kinetics in mixed clay dispersions, Langmuir 27 (9) (2011) 5193–5203.
[243] J. Liu, et al., Synthesis and self-assembly of amphiphilic Janus laponite disks, Macromolecules 46 (15) (2013) 5974–5984.

[244] N. Uchida, et al., Photoclickable dendritic molecular glue: noncovalent-to-covalent photochemical transformation of protein hybrids, J. Am. Chem. Soc. 135 (12) (2013) 4684–4687.
[245] F. Alizadegan, et al., Improving self-healing performance of polyurethane coatings using PU microcapsules containing bulky-IPDI-BA and nano-clay, Prog. Org. Coat. 123 (2018) 350–361.
[246] D. Yang, et al., Color-tunable luminescent hydrogels with tough mechanical strength and self-healing ability, J. Mater. Chem. C 6 (5) (2018) 1153–1159.
[247] Z. You, et al., Nanoclay-modified asphalt materials: Preparation and characterization, Constr. Build. Mater. 25 (2) (2011) 1072–1078.
[248] S.G. Jahromi, A. Khodaii, Effects of nanoclay on rheological properties of bitumen binder, Constr. Build. Mater. 23 (8) (2009) 2894–2904.
[249] E. Santagata, et al., Fatigue and healing properties of nano-reinforced bituminous binders, Int. J. Fatigue 80 (2015) 30–39.
[250] M.J. Khattak, et al., Microstructure and fracture morphology of carbon nano-fiber modified asphalt and hot mix asphalt mixtures, Mater. Struct. 46 (12) (2013) 2045–2057.
[251] E. Santagata, et al., Fatigue and healing properties of bituminous mastics reinforced with nano-sized additives, Mech. Time-Dependent Mater. 20 (3) (2016) 367–387.
[252] J.-J. Wang, et al., Experimental study on self-healing of crack in clay seepage barrier, Eng. Geol. 159 (2013) 31–35.
[253] I. Amin, et al., Laboratory evaluation of asphalt binder modified with carbon nanotubes for Egyptian climate, Constr. Build. Mater. 121 (2016) 361–372.
[254] E. Santagata, et al., Effect of sonication on high temperature properties of bituminous binders reinforced with nano-additives, Constr. Build. Mater. 75 (2015) 395–403.
[255] S.H. Adsul, et al., Self-healing ability of nanoclay-based hybrid sol–gel coatings on magnesium alloy AZ91D, Surf. Coat. Technol. 309 (2017) 609–620.
[256] E.W.K. Loh, D. Chitral Wijeyesekera, Hydraulic flow through engineering bentonite-based containment barriers, Am. J. Appl. Sci. 12 (11) (2015) 785–793.
[257] C. Zúñiga, et al., Self-foaming diphenolic acid benzoxazine, Polymer 53 (15) (2012) 3089–3095.
[258] A. Stimilli, et al., Chemical and rheological analysis of modified bitumens blended with “artificial reclaimed bitumen”, Constr. Build. Mater. 63 (2014) 1–10.
[259] F. Canestrari, et al., Modeling and assessment of self-healing and thixotropy properties for modified binders, Int. J. Fatigue 70 (2015) 351–360.
[260] B.S. Underwood, A continuum damage model for asphalt cement and asphalt mastic fatigue, Int. J. Fatigue 82 (2016) 387–401.